Stem Cell Rev and Rep (2011) 7:815–835
DOI 10.1007/s12015-011-9251-9

Identity, Fate and Potential of Cells Grown as Neurospheres: Species Matters

Carolin Steffenhagen · Sabrina Kraus · Franz-Xaver Dechant · Mahesh Kandasamy · Bernadette Lehner · Anne-Maria Poehler · Tanja Furtner · Florian A. Siebzehnrubl · Sebastien Couillard-Despres · Olaf Strauss · Ludwig Aigner · Francisco J. Rivera

Published online: 24 March 2011

Abstract It is commonly accepted that adult neurogenesis and gliogenesis follow the same principles through the mammalian class. However, it has been reported that neurogenesis might differ between species, even from the same order, like in rodents. Currently, it is not known if neural stem/progenitor cells (NSPCs) from various species differ in their cell identity and potential. NSPCs can be expanded ex vivo as neurospheres (NSph), a model widely used to study neurogenesis in vitro. Here we demonstrate that rat (r) and mouse (m) NSph display different cell identities, differentiation fate, electrophysiological function and tumorigenic potential. Adult rNSph consist mainly of oligodendroglial progenitors (OPCs), which after repeated passaging proliferate independent of mitogens, whereas adult mNSph show astroglial precursor-like characteristics and retain their mitogen dependency. Most of the cells in rNSph express OPC markers and spontaneously differentiate into oligodendrocytes after growth factor withdrawal. Electrophysiological analysis confirmed OPC characteristics. mNSph have different electrophysiological properties, they express astrocyte precursor markers and spontaneously differentiate primarily into astrocytes. Furthermore, rNSph have the potential to differentiate into oligodendrocytes and astrocytes, whereas mNSph are restricted to the astrocytic lineage. The phenotypic differences between rNSph and mNSph were not due to a distinct response to species specific derived growth factors and are probably not caused by autocrine mechanisms. Our findings suggest that NSph derived from adult rat and mouse brains display different cell identities. Thus, results urge for caution when data derived from NSph are extrapolated to other species or to the in vivo situation, especially when aimed towards the clinical use of human NSph.

Keywords Adult neural stem cells · Cell phenotype · Differentiation potential · Cell fate · Glial progenitor cells

Ludwig Aigner and Francisco J. Rivera contribute equally to this study

C. Steffenhagen · M. Kandasamy · T. Furtner · S. Couillard-Despres · L. Aigner (✉) · F. J. Rivera
Institute of Molecular Regenerative Medicine,
Paracelsus Medical University Salzburg,
Strubergasse 21,
Salzburg 5020, Austria
e-mail: ludwig.aigner@pmu.ac.at

C. Steffenhagen · F.-X. Dechant · B. Lehner
Department of Neurology, University of Regensburg,
Regensburg, Germany

S. Kraus · O. Strauss
Department of Ophthalmology, University of Regensburg,
Regensburg, Germany

A.-M. Poehler
Division of Molecular Neurology,
University Hospital of Erlangen,
Erlangen, Germany

F. A. Siebzehnrubl
Department of Neuropathology. Franz-Penzoldt-Center,
University of Erlangen-Nuremberg,
Nuremberg, Germany

Introduction

Adult neural stem and progenitor cells (NSPCs) are currently explored for their potential therapeutic use in degenerative brain diseases and widely used as an in vitro model for neurogenesis. NSPCs can be isolated from the adult brain [1–6] based on the mitogenic activity of

epidermal growth factor (EGF) [4] and/or fibroblast growth factor-2 (FGF-2) [7], which stimulate the formation of floating aggregates, so called neurospheres (NSph) (for review see [6]). NSph are encouraged to differentiate into mature neural cell types by withdrawing the mitogenic growth factors and/or adding specific factors promoting differentiation into particular neural lineages. For example retinoic acid (RA), brain derived neurotrophic factor (BDNF) and neurotrophin-3 (NT-3) induce neuronal differentiation [8, 9], bone morphogenetic protein-2 and −4 (BMP-2/-4) induce astrocytic differentiation [8, 10, 11], while insulin-like growth factor-1 (IGF-1) and mesenchymal stem cell-conditioned media (MSC-CM) promote oligodendroglial differentiation [12, 13].

While neurogenesis was detected virtually in all mammals including humans [14, 15] and NSPCs can be grown from different species, most of the studies related to this topic have been performed in the rodent species rat and mouse. It is generally assumed that mechanisms regulating neurogenesis are well conserved throughout mammals. However, a recent study demonstrated species differences in neurogenesis [16]. In rats, neurogenesis is more efficient and more relevant for certain behavioral aspects than in mice, since newly generated neurons in rats mature faster and contribute more to fear memory as in mice [16]. In addition, a zone in the adult dentate gyrus that lacks newly generated neurons, the so-called neurogenesis quiescent zone, has recently been discovered in adult rats but is apparently absent in mice [17, 18]. Therefore, there are clear species differences in in vivo neurogenesis. In vitro, although NSph are widely used, the issue regarding species differences has never been addressed so far. However, comparing some studies that use NSph as experimental model, species differences can be anticipated. For instance, while stromal cell-derived factor 1 (SDF-1) promotes cell migration in mouse embryo derived NSph [19], it induces cell proliferation in NSph obtained from rat embryos [20]. Also, leukemia inhibitory factor (LIF) induces self-renewal in adult mouse derived NSph-forming cells [21], while there is no effect of LIF on cell proliferation and fate in adult rat derived NSph [22]. Likewise, we have described that mesenchymal stem cells (MSCs) derived soluble factors promote oligodendrocyte fate in cells derived from adult rat (r) NSph [13], however, we did not observe this pro-oligodendrogenic effects in cells derived from adult mouse (m) NSph (Rivera, unpublished observation). It has been shown that adult mouse and rat NSPCs displayed different proliferative and differentiation capacities [23]. Moreover, rodent neural stem cells are different from human neural stem cells in terms of the specific marker expression, the response to growth factors and the timing of isolation (reviewed in [24]). Species dependent differences have also been described for human and mouse embryonic stem cells (ESCs) regarding e.g. morphology, gene expression profile, development and pathways that are involved in ESC self-renewal [25, 26]. Differences in the properties of cells derived from various species might also play a role in the field of plasticity and the generation of chimeric animal models [27, 28].

Here, we aimed to characterize and determine the cell identity of NSph cells derived from adult hippocampi of two different rodent species, rat and mouse. In addition, we provide a comprehensive and descriptive analysis on growth potential, growth factor dependency, tumor potential, differentiation potential and fate, as well as functional electrophysiological data, which taken together present major species differences between adult brain derived mouse and rat NSph.

Materials and Methods

Animal Subjects

Adult female Fischer 344 rats and adult female black C57BL/6 mice (Charles River Deutschland GmbH, Germany) were used as donors for the NSph cultures. All experiments were carried out in accordance with the European Communities Council Directive (86/609/EEC) and institutional guidelines.

Mouse and Rat NSPCs Cultures and NSph Formation

NSPCs derived from the adult hippocampus were generated as described [5, 13]. Hippocampi from 2 to 4 month-old mice or rats (Charles River Deutschland GmbH, Germany) were aseptically removed, transferred to 4°C DPBS (PAN, Germany) with 4.5 g/L glucose (Merck, Germany) (DPBS/glu), washed and mechanically dissected. The cell suspension was washed in DPBS/glu and resuspended in PPD-solution containing 0.01% Papain (Worthington Biochemicals, England), 0.1% dispase II (Boehringer, Germany), 0.01% DNase I (Worthington Biochemicals, England) and 12.4 mM $MgSO_4$ in HBSS (PAN, Germany) without Mg^{++}/Ca^{++} (PAA, Germany) and digested for 30–40 min at 37°C. The cell suspension was triturated every 10 min. Dissociated cells were collected and resuspended in Neurobasal (NB) media containing 1 × B27 (Gibco BRL, Germany; detailed formulation see [5]), 2 mM L-glutamine and 100 U/mL penicillin/100 µg/ml streptomycin and washed and cells were resuspended in NB media (Gibco BRL, Germany) supplemented with 1 × B27 (Gibco BRL, Germany), 2 mM L-glutamine (PAN, Germany), 100 U/mL penicillin/100 µg/ml streptomycin (PAN, Germany), 2 µg/ml heparin (Sigma, Germany), 20 ng/ml human recombinant bFGF-2 (R&D Systems GmbH, Wiesbaden-Nordenstadt, Germany) and 20 ng/ml human recombinant EGF (R&D Systems

GmbH, Wiesbaden-Nordenstadt, Germany). Alternatively, rat or mouse derived single cell suspension was incubated with 20 ng/ml rat or mouse recombinant bFGF-2 (R&D Systems GmbH, Wiesbaden-Nordenstadt, Germany) and/or 20 ng/ml rat or mouse recombinant EGF (R&D Systems GmbH, Wiesbaden-Nordenstadt, Germany), respectively. Cultures were maintained at 37°C in an incubator with 5% CO_2. Half of the media was changed every 3–4 days. After 1–2 weeks NSPCs form NSph. In general, cultures from passage number 2–6 (low passage) were used throughout this study. For long-term culture experiments passage number 25–29 (high passage) were used.

MSCs Culture

MSCs were prepared as described previously [13]. Briefly, bone marrow plugs were harvested from femurs and tibias from 2 to 4 month-old female Fisher-344 rats (Charles River Deutschland GmbH, Germany). Plugs were mechanically dissociated in αMEM (Gibco Invitrogen, Karlsruhe, Germany) and recovered by centrifugation. Cell pellets were resuspended in αMEM-10% fetal bovine serum (FBS) and seeded at 1×10^6 cells/cm^2. After 3 days, media was changed and non-adherent cells were removed. Adherent cells were incubated in fresh αMEM-10% FBS until a confluent layer of cells was achieved. Cells were trypsinized using 0.25% Trypsin (Gibco Invitrogen, Karlsruhe, Germany) and seeded in αMEM-10% FBS at 8,000 cells/cm^2. After 3–5 days of culture, the resulting monolayer of cells, hereafter named rat bone marrow derived MSCs, was trypsinized and further cultured for experiments or frozen for later use. As demonstrated in our previous work, this cell culture preparation is highly enriched in multipotent MSCs with virtually no hematopoietic contamination [13].

Cell Number Analysis

For estimating proliferation of NSph by assessing cell number, 5×10^4 cells/well were seeded into 6-well plates with a volume of 2 ml NB media. Cells were grown for 1 week and cell number was determined after 1, 3, 5 and 7 days. For that, the cells were treated with Trypan blue (Sigma-Aldrich, Taufkirchen, Germany). Subsequently, the number of living cells was determined using a light microscope (Zeiss, Germany). Media was changed after 4 days.

Cell Cycle Analysis

The cell cycle was analyzed by fluorescence activated cell sorting (FACS) using a modified Ki67/PI staining protocol from Endl and colleagues [29]. NSph derived from adult hippocampus were seeded into T75 flasks (TPP, Switzerland) and grown under proliferative conditions. After 1 or 2 weeks, cells were spun down, medium was removed and cells were fixed with 1 ml ice cold 70% EtOH. After fixation cells were washed with ice cold PBS and then resuspended in 500 μl ice cold PBS containing 0.1% TritonX-100 and incubated for 5 min on ice. After 2 subsequent washing steps, cells were resuspended in 100 μl of a 1:6 dilution of the antibodies in PBS (100 μl PBS + 20 μl antibody IgG or Ki67 BD Biosciences Pharmingen, FITC conjugated antibodies). After 30–40 min incubation at 4°C, cells were washed with 15 ml PBS and then resuspended in PBS for staining. In case of PI staining, cells were resuspended in 470 μl PBS. Cells without PI staining were resuspended in 495 μl. All samples were treated with 5 μl of RNase for 1 h to eliminate the RNA, which would interfere with the PI staining. After this 1 h incubation at 37°C, 25 μl of PI were added to the respective samples. The stained cells were analyzed with the Flow Cytometer (FACS Calibur, Becton Dickinson, Heidelberg). Data were analyzed using Win MDI 2.8 software.

Conditioned Media Preparation

MSC-CM was prepared similar as described [13]. MSCs were plated at 12,000 cells/cm^2 and incubated in DMEM Knockout-20% Serum Replacement supplement (SR). After 3 days, the conditioned media was collected and filtered using a 0.22 μm-pore filter and used as a NSPCs oligodendrogenic stimulus.

Species-specific NSph conditioned media was prepared by plating rat or mouse NSph at a density of 5×10^5 cells/cm^2 in NB media into T75 culture flasks. After 3–5 days, the supernatant was collected and filtered using a 0.22-μm-pore filter. These filtrates were termed rNSph- and mNSph-conditioned media (rNSph-CM; mNSph-CM).

Expression Profile Analysis of Cell-Lineage-Specific Markers

Spheres were dissociated with Accutase (Innovative Cell Technologies Inc., distributed by PAA) and plated on 100 μg/ml poly-L-ornithine (Sigma-Aldrich, Taufkirchen, Germany) and 5 μg/ml laminin-coated (Sigma-Aldrich, Taufkirchen, Germany) glass coverslips at a density of 2.5×10^4 cells/cm^2 in DMEM Knockout-20% SR (Gibco Invitrogen, Karlsruhe, Germany) for 12 h. This serum-free media has been used for ESC maintenance and does not induce differentiation [30–32]. Under these conditions dissociated NSph attach to the plate in the absence of serum. Finally, cells were fixed for 30 min with 4% paraformaldehyde and processed for immunofluorescence to analyze the expression of cell specific markers.

Growth Factor Withdrawal and Serum-Free Conditions Response

To analyze the response to growth factor withdrawal (GFW) under serum-free conditions, proliferating NSph in the presence of FGF-2 and EGF were dissociated with Accutase and plated as described in the previous section. Cells were incubated in DMEM Knockout-20% SR (Gibco Invitrogen, Karlsruhe, Germany) without growth factors and in the absence of serum. After 7 days, cells were fixed for 30 min with 4% paraformaldehyde and processed for immunofluorescence to detect the expression of the different cell specific markers tested.

Differentiation Assay of Adult NSph and Serum Response

To assess the differentiation potential of adult rNSph and mNSph, $2–5\times10^4$ cells/well were plated on 100 μg/ml poly-L-ornithine (Sigma-Aldrich, Taufkirchen, Germany) and 5 μg/ml laminin-coated (Sigma-Aldrich, Taufkirchen, Germany) glass coverslips into 24-well plates in DMEM Knockout-20% SR (Gibco Invitrogen, Karlsruhe, Germany). After 12 h, the media was refreshed with DMEM Knockout-20% SR, with MSC-CM or with DMEM Knockout-20% SR supplemented with the tested differentiation factors: 2 μM RA (Sigma-Aldrich, Taufkirchen, Germany) and 10 ng/ml BMP-2 and BMP-4 (R&D Systems GmbH, Wiesbaden-Nordenstadt, Germany). Alternatively, in order to analyze serum response media was supplemented with 10% FBS (PAN Biotech GmbH, Aidenbach, Germany). Media were refreshed every third day. After 7 days, the cells were fixed for 30 min with 4% paraformaldehyde and processed for immunofluorescence staining.

Cross-Incubation with Species-Specific Conditioned Media

To test the effect of conditioned media derived from rNSph and mNSph on adult rNSph and mNSph, cells were incubated up to 3 weeks with conditioned media from the other species (cross), i.e. mouse derived NSph were incubated with 2/3 rNSph-CM and 1/3 fresh media, while rat derived NSph were incubated with 2/3 mNSph-CM and 1/3 fresh media. Media was changed every 3–4 days and after 7 days the NSph cultures were passaged like before mentioned. After incubation period NSph were dissociated and markers expression profile and growth factor withdrawal response were analyzed as previously described.

Cell-Lineage Commitment Analysis

rNSph and mNSph derived cells were incubated under proliferation conditions, i.e. in NB media or in NB media supplemented with 1 μg/ml sonic hedgehog (Shh), 50 ng/ml Noggin, 20 ng/ml platelet-derived growth factor AA homodimer (PDGF-AA), 10 ng/ml BMP-2 and BMP-4 (all from R&D Systems GmbH, Wiesbaden-Nordenstadt, Germany), 20 ng/ml T3 (Sigma-Aldrich, Taufkirchen, Germany). Media was changed every 3–5 days and after 7 days the NSph cultures were passaged. After 3 weeks of incubation, NSph were dissociated and markers expression profile and growth factor withdrawal response were analyzed as previously described.

Immunocytochemistry

Fixed cells were washed in TBS (0.15 M NaCl, 0.1 M Tris–HCl, pH 7.5), then blocked with solution composed of TBS, 0.1% Triton-X100 (only for intracellular antigens), 1% bovine serum albumin (BSA) and 0.2% Teleostean gelatin (Sigma, Germany) (fish gelatin buffer, FGB). The same solution was used during the incubations with antibodies. Primary antibodies were applied overnight at 4°C. Fluorochrome-conjugated species-specific secondary antibodies were used for immunodetection. The following antibodies and final dilutions were used. Primary antibodies: rabbit anti-GFAP 1:1000 (Dako, Denmark); mouse anti-rat Nestin 1:500 (Pharmingen, Heidelberg, Germany); IgM mouse anti-O4 1:100 (Chemicon, USA); IgM mouse anti-A2B5 1:200 (Chemicon, UK); rabbit anti-platelet-derived growth factor receptor alpha (PDGFRα) 1:100 (Santa Cruz, Heidelberg, Germany); mouse anti-Map 2a+2b 1:250 (Sigma, Germany); rabbit anti-doublecortin (DCX) 1:500 (NEB, Frankfurt, Germany); mouse anti-Myelin Basic Protein (MBP) 1:750 (SMI-94, Sternberger Monoclonals Incorporated, U.S.A.). Secondary antibodies: donkey anti-mouse, rabbit conjugated with Alexa Fluor 488 (Molecular Probes, Eugene, OR, USA), rhodamine X 1:1000 (Dianova, Hamburg, Germany). In cases of detergent-sensitive antigens (i.e. O4, A2B5 and PDGFRα), Triton X-100 was omitted from FGB buffer. Nuclear counterstaining was performed with 4′, 6′-diamidino-2-phenylindole dihydrochloride hydrate at 0.25 μg/μl (DAPI; Sigma, Germany). Specimens were mounted on microscope slides using Prolong Antifade kit (Molecular Probes, U.S.A.). Epifluorescence observation and photo-documentation were realized using a Leica microscope (Leica Mikroskopie und Systeme GmbH, Germany) equipped with a Spot™ digital camera (Diagnostic Instrument Inc, U.S.A.). For each culture condition, 10 randomly selected observation fields, containing in total 500–1,000 cells, were photographed for cell fate analysis. Expression frequency of selected cell type markers was determined for every condition in three independent experiments.

Chromosome Preparation

NSph cultures were incubated with Colcemid (0.4 μg/ml) for 3 h and then treated with Accutase for 10 min at 37°C. Cells were centrifuged and the pellet was suspended in warm hypotonic solution (0.075 M KCl in H_20) for 10 min at 37°C. After centrifugation the cells were fixed in a 3:1 mixture of cold methanol-glacial acetic acid for 30 min. In order to prepare the metaphase spreads the cell suspension was dropped on glass slides, dried and Giemsa stained. 20–25 metaphase spreads were analyzed for the number of chromosomes and for chromosomal aberrations.

Quantitative PCR

RNA extraction from adult rNSph and mNSph was performed using RNeasy Mini Kit (Qiagen, Hilden, Germany) and cDNA was synthesized using Promega reverse transcription Kit (Promega). Expression analysis was performed by TaqMan gene expression assays kits (Applied Biosystems, California, USA) for the following genes: rat Sox2, mouse Sox2, rat Hes1, mouse Hes1, rat Neurogenin1, mouse Neurogenin1, rat Olig1, mouse Olig1, rat Olig2 and mouse Olig2. Probes and primers for each gene were provided by manufacturer (Applied Biosystems, California, USA). Rat and mouse Glyceraldehyde 3-phosphate dehydrogenase (GAPDH) as well as Beta-2-microglobulin (B2M) were used as endogenous control genes. The following temperature profile was used: activation of polymerase 95°C, 10 min; 40 cycles of denaturing 95°C, 15 s, and annealing/extension 60°C, 60 s. Data were obtained with a Rotor-Gene 6000 R Corbett Research (geneXpress, Vienna, Austria) and analyzed by delta delta Ct method [33]. Olig 1 was used as calibrator since from all genes tested this was the highest expressed in both cell types. Finally, the expression value of Sox 2, Hes 1, Olig 2 and Neurogenin 1 was determined for each species.

Electrophysiological Recordings

For electrophysiological recordings, NSph were dissociated and seeded overnight on poly-L-ornithine/laminin-coated coverslips in DMEM Knockout-20% SR. Recordings of membrane currents were performed using the whole-cell patch-clamp technique at room temperature (22–25°C). Coverslips with adherent rNSph and mNSph cells were placed in a perfusion chamber mounted onto the stage of an inverted microscope: The cells were superfused with a standard bath solution containing (in mM): 130 NaCl, 3 KCl, 4 $MgCl_2$, 1 $CaCl_2$, 2,5 EGTA, 10 HEPES and 5 glucose, adjusted to pH 7,4 with NaOH. Studies of Na^+ currents were performed in a K^+-free bath solution consisting of (in mM): 125 NaCl, 0.5 $CaCl_2$, 10 $BaCl_2$, 4 $MgCl_2$, 2.5 EGTA, 10 HEPES, 5 glucose, adjusted to pH 7.4 with NaOH.

Patch–clamp electrodes were pulled from borosilicate glass tubes using a Zeitz DMZ Universal Puller (Zeitz, Augsburg, Germany) and showed a resistance of 3–5 MΩ. Pipettes were filled with a intracellular solution containing (in mM): 140 KCl, 2 $MgCl_2$, 1 $CaCl_2$, 2,5 EGTA, 10 HEPES and 3 ATP, adjusted to pH 7,4 with KOH.

For studying Na^+ currents, KCl in the pipette solution was entirely replaced by CsCl and 1 mM Ba^{2+} was added to the bath solution. TTX (100 nM) was added to the standard solution as indicated. Current traces were recorded before and after the application of TTX (10 nM) and subtracted to isolate the TTX-sensitive component. No changes in cell size were observed during the whole-cell configuration with these solutions.

All recordings were made with a HEKA EPC 10 amplifier (HEKA Electronic, Lamprecht, Germany). TIDA software (HEKA Electronic, Lamprecht, Germany) was used for electrical stimulation as well as for data acquisition and analysis. In general, voltage-dependent currents were activated using a voltage-step protocol consisting of voltage steps of 10 mV increasing amplitude and 50 ms duration to depolarize cells from the indicated holding potential (−40 mV for K^+ currents measuring and −80 mV for Na^+ recordings). The membrane capacitance and access resistance were compensated after the whole-cell configuration was established. The access resistance was compensated for values lower than 10 MΩ. The resting potential was measured directly after establishing the whole-cell configuration and before membrane capacitance or access resistance was compensated. For analysis of voltage-dependent activation steady-state currents were plotted against the membrane potentials of the electrical stimulation. Current densities were expressed as the ratio between maximal current amplitude and whole-cell membrane capacitance (pA/pF) at given voltage depolarizations.

Statistical Analysis

Electrophysiological data are presented as means ± SEM for the indicated number of independent measurements (n). Statistical analyses were performed using SigmaPlot 10 (Systat Software Inc., Richmond, CA). The rest of the data are presented as means ± SD and statistical analysis was performed using PRISM4 (GraphPad, San Diego, CA, USA). Depending on the experiment performed, significance was acquired by Mann–Whitney U non-parametric test, parametric two-tailed *t*-test, one-way ANOVA-Tukey post hoc or two-way ANOVA-Bonferroni post hoc. All experiments were performed in

triplicate or more and P values of <0.05 were considered to be significant.

Results

rNSph and mNSph Differ in Their Substrate Adherence and Proliferation Rate

NSPCs were derived from hippocampus of adult rat and mouse brains and cultured as NSph as described before [5, 13]. Special care was taken in following exactly the same protocol and procedure of hippocampal dissection and preparation of the cultures between the two species. rNSph grew as floating aggregates, while mNSph aggregates mostly attached to the plastic surface of the culture dish, only some aggregates were free floating (Fig. 1a, b). The analysis of the growth kinetic over a period of 1 week showed that mNSph had a higher growth rate compared to rNSph (Fig. 1c). However, the overall growth dynamic after splitting and reseeding was comparable between the two species and consisted of a lag phase, an expansion phase from day 3 to day 5 and finally a trend to reach a plateau after 1 week (Fig. 1c). The percentage of cells in cell cycle (G_1S-G_2M) was significantly higher in mNSph, and vice versa, the percentage of cells in cell cycle exit (G_0) was significantly lower in mNSph cultures (Fig. 1d). Thus, the higher growth rate found in the mNSph culture is probably due to a higher proportion of cells that are in cell cycle compared to the rNSph culture. In summary, mNSph and rNSph display different adherent properties and proliferation capacities.

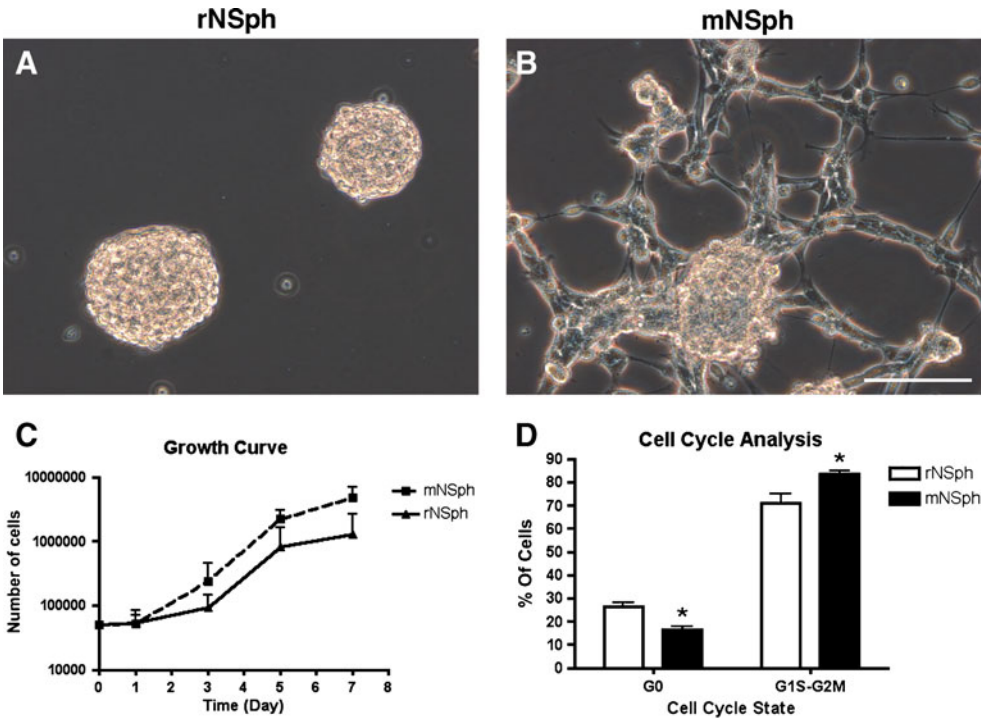

Fig. 1 Rat and mouse derived NSph displayed different morphologies, adherent properties and proliferation capacities. (**a**, **b**) Phase contrast images of proliferating NSph. When rNSph and mNSph were cultured in the presence of growth factors, rNSph grew as floating aggregates (**a**), while mNSph mainly attached to the substratum and only some mNSph were free floating (**b**). Scale bar = 100 μm. (**c**) Cell counting of NSph after day 1, 3, 5 and 7 to define characteristic growth curves. Both rNSph and mNSph show similar growing kinetics but mNSph display a higher growth rate than rNSph. (**d**) FACS analysis for the different NSph types. mNSph displayed less cells in G_0 state and more in G_2-M. For statistical analysis, Two-way ANOVA-Bonferroni post hoc test was performed (* = $p<0.05$)

Fig. 2 rNSph and mNSph display different phenotypes. (**a**, **b**) Phase contrast images of dissociated NSph. rNSph (**a**) and mNSph (**b**) were dissociated and seeded in differentiation media without serum. Scale bar = 100 μm. (**d**, **e**, **g**, **f**, **j**, **k**, **m**, **n**) Fluorescence images of Nestin/GFAP/DAPI (**d**, **e**), A2B5/DAPI (**g**, **h**), O4/DAPI (**j**, **k**) and DCX/DAPI (**m**, **n**) for rNSph (*left row*) and mNSph (*right row*). Scale bar = 50 μm. (**f**, **i**, **l**, **o**) Quantitative analysis of the marker expression of NSph under proliferation conditions. mNSph highly expressed the neural stem cell/astrocyte markers Nestin and GFAP (**f**), while they showed weak expression for A2B5 (**i**), O4 (**l**) DCX (**o**). In contrast, rNSph expressed significantly more the glial marker A2B5 (**i**) and the oligodendroglial marker O4 (**l**) than mNSph. But the number of Nestin + and GFAP + cells (**f**) was very low in rNSph. Surprisingly, a significant amount of DCX-expressing cells was found in rNSph, but they mainly displayed an OPC morphology. For statistical analysis, Student *t*-test and two-way ANOVA-Bonferroni post hoc test were performed (*** = $p<0.001$). (**c**) Quantitative RT-PCR for cell fate determinants, Sox 2 and Hes 1 were used as astrocyte determinants while Olig 2 as oligodendrocyte determinant. A higher (Sox 2 + Hes 1)/Olig2 ratio was observed in mNSph compare to rNSph. For statistical analysis Mann–Whitney U non-parametric test was performed (*** = $p<0.001$). Abbreviations: *OPC* Oligodendrocyte Progenitor Cells

rNSph and mNSph Display Differences in Their Phenotypes, Cell-Intrinsic Fates and Differentiation Potentials

Single adherents cells derived from rat and mouse NSph displayed different cell morphologies. While rat cells had a multipolar morphology with primary process and secondary branches, mouse cells displayed a pyramidal morphology with no secondary branches (Fig. 2a, b). In addition to this, the cells displayed a different cell-lineage-

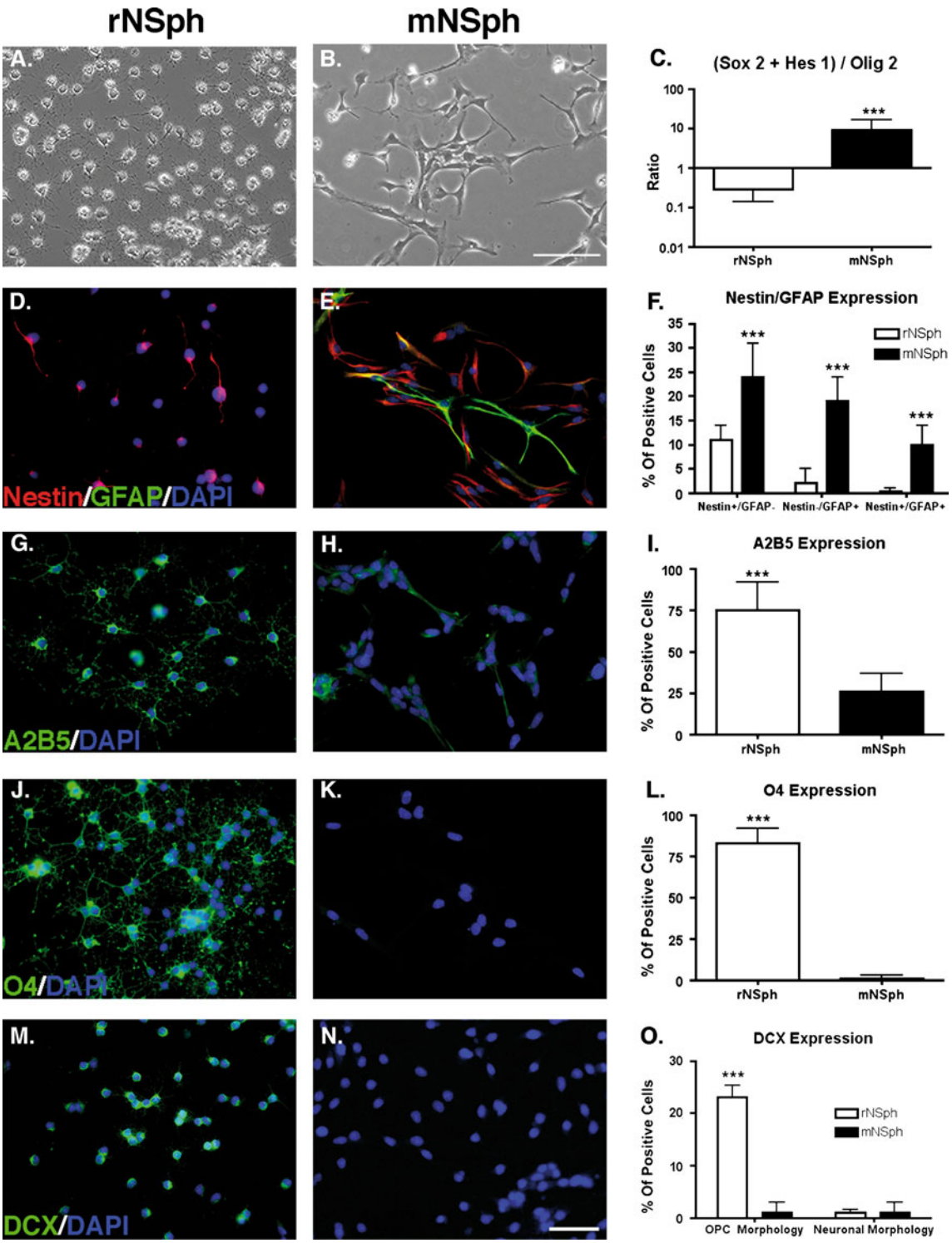

specific marker expression profile. While most of the cells derived from mNSph expressed the neural stem cell/astrocyte markers Nestin and/or GFAP, just a few rat cells expressed these markers (Fig. 2d–f). Conversely, most of the cells derived from rNSph expressed the glial progenitor marker A2B5 (Fig. 2g–i) and the oligodendroglial progenitor marker O4 (Fig. 2j-l), while only a few mouse cells expressed these markers. Surprisingly, a relatively high proportion of rNSph but not mNSph derived cells expressed the neuroblast and neuronal precursor marker DCX, even though these were cells with an oligodendroglial progenitor morphology (Fig. 2m–o). There were virtually no DCX-expressing cells with an elaborated neuronal morphology in the two cultures (Fig. 2m–o). In

addition, under proliferation conditions neither rNSph nor mNSph expressed mature oligodendroglial or neuronal markers as indicated by absence of MBP or Map2ab immunoreactivtiy. While rNSph cells did not express the astrocyte/stem cell marker GFAP, some cells (14.6% ± 0.5) derived from mNSph did (data not shown).

In summary, rNSph derived cells mostly express markers that are considered to be specific for oligodendroglial progenitors, while the DCX expression in these cells suggests also a potential for neuronal fate. In contrast, mNSph derived cells seem to have an astrocytic/stem cell identity. This is further supported by the expression pattern of neural stem cell/astroglial/oligodendroglial cell fate determinants as revealed by quantitative RT-PCR analyses. While mNSph express more of the neural stem cell/astrocyte determinants Sox2 and Hes1, rNSph express relatively more of the oligodendroglial determinant Olig2 (Fig. 2c).

In order to determine the cell intrinsic fate of rNSph and mNSph derived cells under non-proliferative conditions, NSph were dissociated, seeded in media that allows survival of NSph derived cells under serum free conditions and after growth factor withdrawal (GFW). The morphological analysis revealed that rNSph derived cells were multipolar with several processes and secondary branches, while mNSph derived cells were flat with a more fibroblastic morphology devoid of elaborated processes (Fig. 3a, b). Most of the cells derived from mNSph spontaneously differentiated into GFAP-expressing astrocytes while almost none of them gave rise to MBP-expressing oligodendrocytes (Fig. 3d, e, g, h). In contrast, most of the cells derived from rNSph spontaneously generated MBP-expressing oligodendrocytes and virtually no GFAP-expressing astrocytes (Fig. 3c, e, f, h). Surprisingly, while none of the rNSph derived cells expressed DCX after 1 week of GFW, a minor percentage of mNSph derived cells generated DCX-expressing cells with a neuronal morphology (Fig. 3i–k). In summary, rat NSph derived cells had an intrinsic commitment to oligodendroglial fate, while mNSph derived cells predominantly displayed an intrinsic fate towards astrogenesis.

Next, we tested the differentiation potential of NSph derived cells in response to various differentiation stimuli. NSph derived cells were grown for 1 week under non-proliferative conditions (GFW) supplemented with distinct stimuli and analyzed for the expression of neuronal and glial markers. First, we used FBS as an undefined trigger for astroglial differentiation [34]. FBS increased the percentage of GFAP-expressing astrocytes in both species (Fig. 4a). This was at the expense of MBP-expressing oligodendrocytes, at least in rNSph derived cells (Fig. 4b). FBS decreased the proportion of DCX-expressing cells in mNSph derived cells (Fig. 4c). Secondly, we tested the response pattern of NSph derived cells to specific astrogenic, oligodendrogenic and neurogenic stimuli. Treatment of NSph derived cells with BMPs, which are known to induce astroglial differentiation [10], resulted in an increase of GFAP-expressing astrocytes in rNSph derived cells, whereas it did not further increase the percentage of GFAP-expressing cells in the mouse cultures (Fig. 4d). Treatment with the pro-oligodendrogenic MSC-CM [13] did neither enhance the already high percentage of MBP-expressing cells in rNSph derived cultures, nor was it able to induce MBP expression in mouse cultures (Fig. 4e). The neurogenic stimulus RA [9] did neither induce the expression of the neuronal marker Map2ab in rNSph derived cells, nor enhance the percentage of Map2ab-expressing cells in the mouse cultures (Fig. 4f). In summary, while rNSph derived cells can be induced to generate oligodendrocytes and astrocytes, mouse cultures predominantly gave rise to astrocytes regardless of the stimulus provided. In addition, in both species a minor population of cells generated Map2ab-positive neurons.

Fate Restriction in Mouse NSph

Often, the fate of progenitors is determined early while cells are still proliferating. Now, we asked whether the intrinsic fate of proliferating rat and mouse NSph can be changed by external stimuli and to what degree these cells are restricted to this fate. For that, rNSph were incubated under proliferation conditions for 3 weeks with BMPs, which are known to promote astrogenesis [10], and mNSph were incubated for 3 weeks with PDGF-AA, T3, Noggin or Shh, factors that are known to promote oligodendroglial fate [35–41]. NSph were then dissociated and cells were seeded to analyze their phenotype and their intrinsic fate in response to GFW. Interestingly, the percentage of rNSph derived cells that expressed O4 after treatment with BMPs was significantly lower compared to the untreated rNSph, a level that was similar to that observed in mNSph (Fig. 5a). However, the expression of GFAP was not increased in response to BMPs treatment (Fig. 5b). Nevertheless, after GFW, the percentage of GFAP-expressing cells was increased, while the proportion of MBP-positive cells was significantly diminished (Fig. 5c, d). Therefore, stimulation with BMPs under proliferation conditions converted rNSph into mouse-like NSph suggesting a low degree of cell-lineage restriction in rNSph.

We also tried to use oligodendrogenic factors with the aim to interconvert mNSph into rat-like NSph. First, we showed that mNSph express PDGFRα (Fig. 5i). Stimulation with PDGF-AA, however, did not affect the phenotype and the intrinsic fate of mNSph. In addition, the oligdendroglial inducers Noggin, Shh and T3 did neither change the expression profile of cell lineage

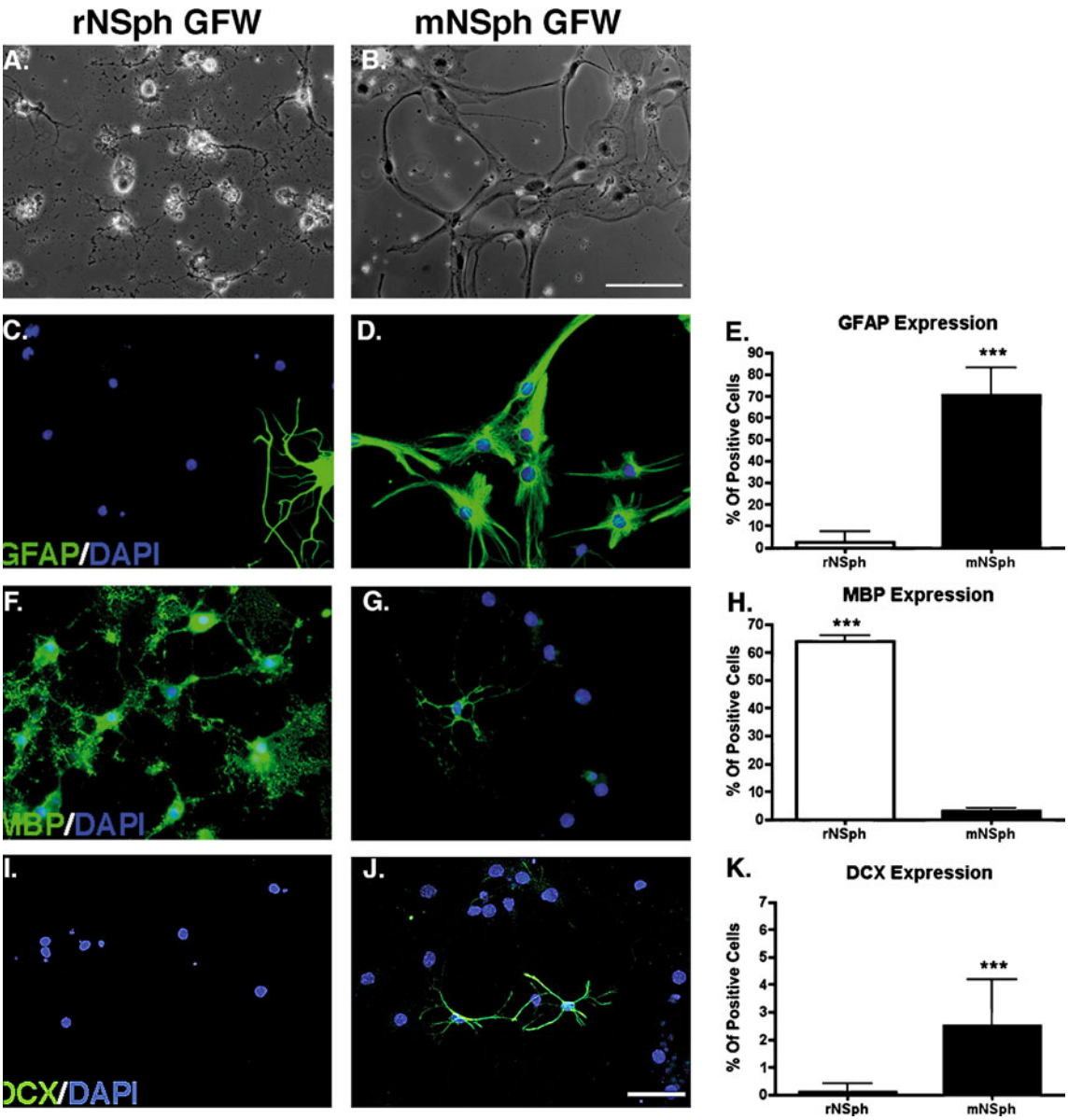

Fig. 3 rNSph and mNSph show different cell fates. (**a**, **b**) Phase contrast images of NSph after 7 days in differentiation media. rNSph (**a**) and mNSph (**b**) were incubated for 1 week in differentiation media without growth factors. Scale bar=100 μm. (**c**, **d**, **f**, **g**, **i**, **j**) Fluorescence images of GFAP/DAPI (**c**, **d**), MBP/DAPI (**f**, **g**) and DCX/DAPI (**i**, **j**) for rNSph (*left row*) and mNSph (*right row*). Scale bar = 50 μm. (**e**, **h**, **k**) Quantitative analysis of the marker expression of rNSph and mNSph under differentiation conditions. rNSph differentiated into MBP-expressing mature oligodendrocytes (**h**) after growth factor withdrawal and showed very weak expression for GFAP (**e**) and DCX (**k**), whereas mNSph differentiated into GFAP-expressing astrocytes (**e**) and some DCX + neurons (**k**), but not into MBP + oligodendrocytes (**h**). For statistical analysis, Student *t*-test was performed (*** = $p<0.001$). Abbreviations: *GFW* growth factor withdrawal

markers, nor did they affect the GFW response of mNSph (Fig. 5e–h). Moreover, the combinatory treatment with different oligodendrogenic factors did neither change the marker expression nor the GFW response of mNSph (Fig. 5e–h). Taken together, proliferating mNSph did not respond to pro-oligodendrogenic factors and retained their predominant intrinsic astroglial fate. In conclusion, mNSph are more restricted to their intrinsic lineage compared to rNSph, which can interconvert between oligodendroglial and astroglial fate.

Long-Term Expansion Induces Transformation in Rat but not in Mouse NSph

Recently, we demonstrated that rNSph derived from the adult subventricular zone (SVZ) spontaneously transform into tumorigenic cell lines upon long-term in vitro expansion and become growth factor independent in their proliferation [42]. Here, we tested whether this is a general phenomenon observed in all NSph cultures regardless of the species. Therefore, we expanded NSph derived from

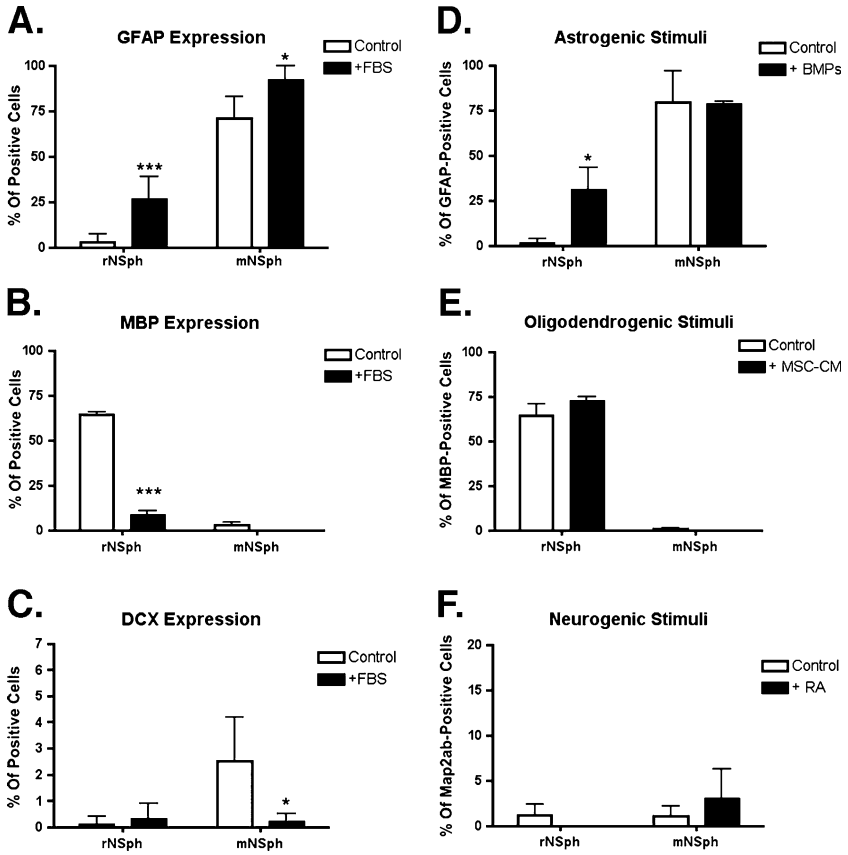

Fig. 4 rNSph and mNSph display different differentiation potentials. Quantitative analysis of the marker expression of NSph in response to FBS (**a**, **b**, **c**) as well as to astrogenic (**d**), oligodendrogenic (**e**) and neurogenic stimuli (**f**). FBS shifted the differentiation of rNSph towards GFAP-expressing astrocytes (**a**) at the expense of MBP-expressing oligodendrocytes (**b**). FBS did not affect DCX expression of rNSph, while it slightly decreased the number of DCX + neurons in mNSph (**c**). FBS also slightly increased the expression of GFAP in mNSph (**a**), but it had no effect on the expression of MBP (**b**). BMPs increased the expression of GFAP in rNSph, while the number of GFAP + astrocytes could not be further enhanced (**d**). Similarly, the expression of MBP could not be further increased through MSC-CM in rNSph (**e**). MSC-CM could not induce MBP expression in mNSph (**e**) like RA could not induce DCX expression in rNSph and mNSph (**f**). For statistical analysis, two-way ANOVA-Bonferroni post hoc test was performed (* = $p<0.05$; *** = $p<0.001$)

adult rat and mouse hippocampus and analyzed the growth factor dependency in low (p2–6) and in high (p25–29) passage cultures. In low passage cultures, proliferation of NSph from both species required the presence of EGF/FGF (Fig. 6a, c). In contrast, in high passage cultures, mNSph retained the growth factor dependency, while rNSph acquired the ability to proliferate in the absence of EGF/FGF (Fig. 6b, d). Even though rNSph cells transformed into tumor-like cells in higher passage, the morphology of rNSph cells did not change (data not shown).

Since the growth factor independence/tumorigenic potential could be due to genetic abnormalities, we analyzed the karyotype of NSph cultures (Fig. 6e). The median chromosome numbers of mNSph in low and high passage cultures were 40 and 37.2, respectively (Table 1), with 40 being the normal number of a diploid mouse chromosome set. In contrast, rNSph low passage cultures were polyploid (Fig. 6e) and showed a mean chromosome number of 67.1 (Table 1), instead of 42 chromosomes being the normal diploid set in rats. Interestingly, rNSph high passage cultures were mainly diploid or pseudodiploid with a mean chromosome number of 39.5 (Table 1). Taken together, the karyotype of mNSph seems to be more stable with only few chromosomal aberrations compared to rNSph, which show a huge heterogeneity regarding their ploidy. In addition, individual chromosomes in the rNSph preparation typically showed a number of deletions, strand breaks and gaps (Fig. 6e). In summary, mNSph, although they show a higher growth kinetic, seem to be somehow protected from spontaneous transformation. Moreover, it shows that spontaneous transformation is not a general attribute to neural progenitor cultures.

rNSph and mNSph Show Different Electrophysiological Properties

Next, we functionally characterized NSph derived from the two different rodent species by investigating their electro-

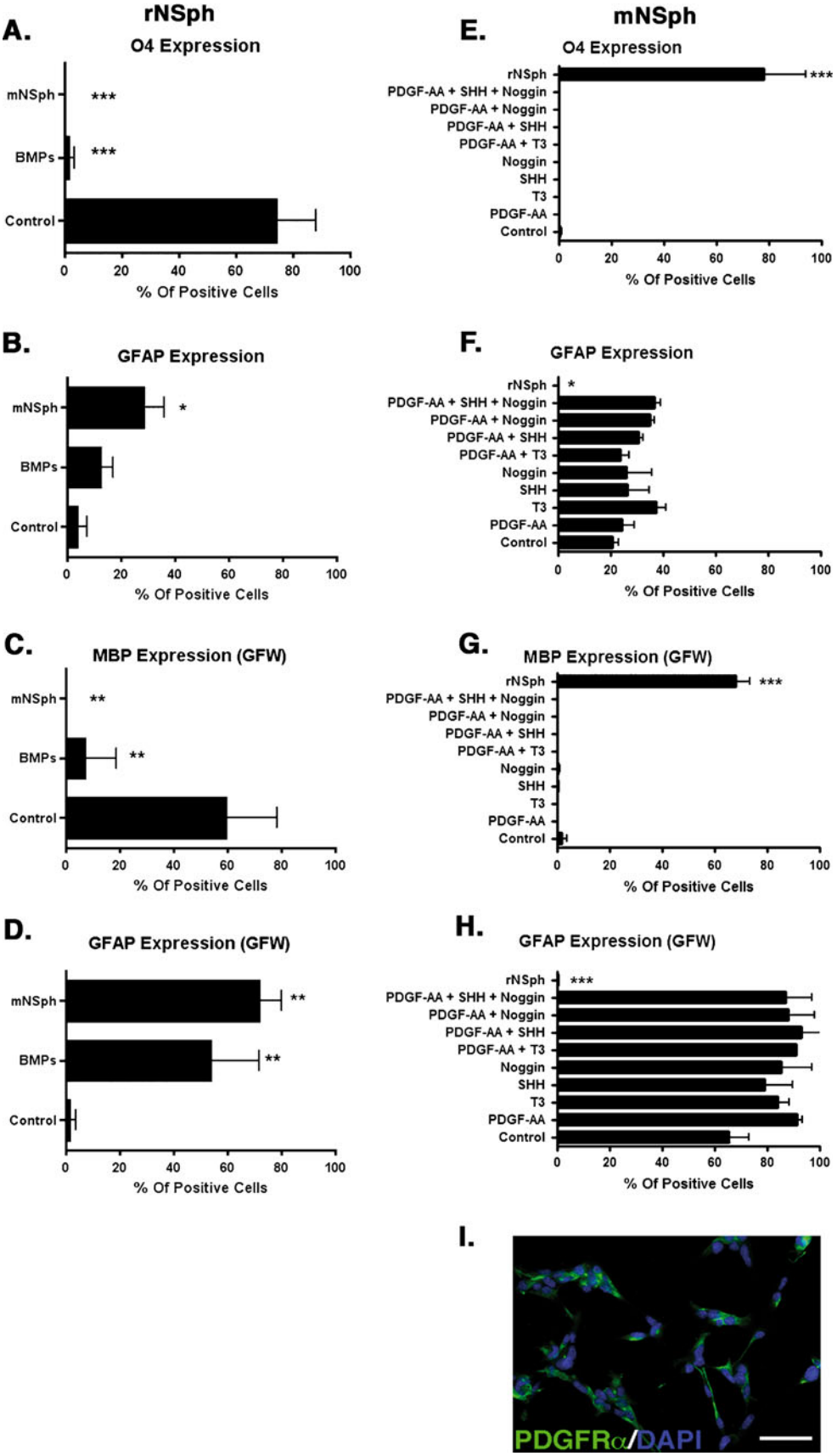

Fig. 5 BMPs induced an astrocyte precursor phenotype on rNSph, while PDGF-AA, Noggin, T3 and Shh could not induce an oligodendroglial progenitor-like phenotype on mNSph. rNSph were incubated for 3 weeks with astrogenic BMPs and mNSph with several oligodendrogenic factors. (**a**, **b**, **e**, **f**) Cell phenotype was analyzed by the expression of cell-lineage-specific markers. (**c**, **d**, **g**, **h**) Cell fate was analyzed by GFW response. BMPs treatment blocked the O4 expression in rNSph compared to control (**a**), while it did not enhance GFAP expression under proliferation conditions (**b**). But in response to GFW, BMPs increased the number of GFAP-positive cells in rNSph at the expense of MBP-positive cells (**d**, **c**). The tested oligodendrogenic factors alone or in combination did not change the cell phenotype and the cell fate of mNSph, since they neither increased the expression of O4 and MBP (**e**, **g**) nor decreased the expression of GFAP compared to control (**f**, **h**). For statistical analysis one-way ANOVA-Tukey post hoc test was performed (* = $p<0.05$, ** = $p<0.01$, *** = $p<0.001$). (I) Fluorescence image for PDGFRα/DAPI showing dissociated PDGFRα-positive mNSph. Scale bar = 50 μm. Abbreviations: *GFW* growth factor withdrawal

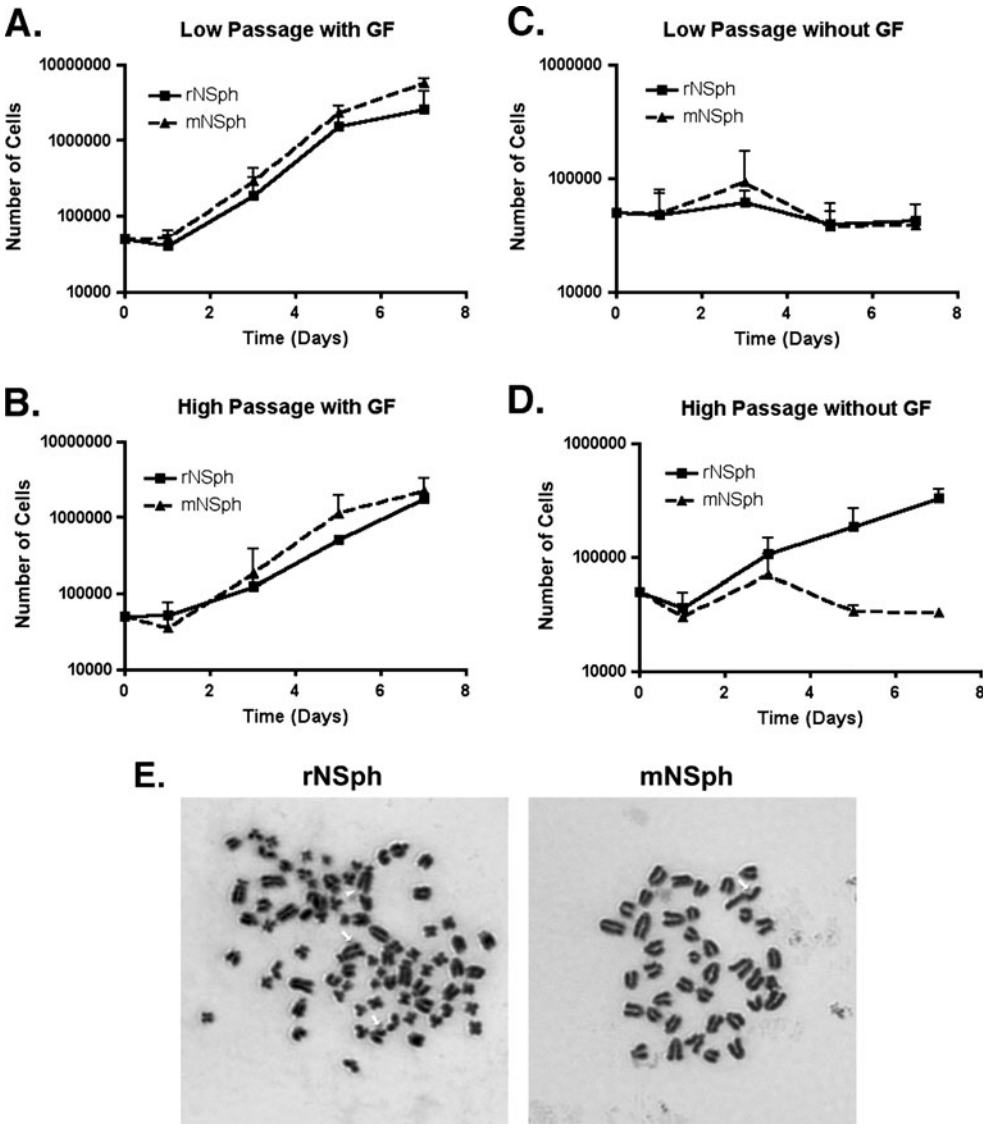

Fig. 6 Rat and mouse derived NSph have different transformations properties. Growth properties and karyotypes from NSph in low (p2–6) and high passage (p25–29) were analyzed. Rat and mouse derived NSph were grown for 7 days in the presence (**a**, **b**) or absence (**c**, **d**) of growth factors. Growth curves were determined for rat and mouse derived NSph with low (p2–6) (**a**, **c**) and high (p25–29) (**b**, **d**) passage number. Note that at low passage number proliferation of rat and mouse cells strictly depended on the presence of growth factors but at high passage number rat cultures became growth factor independent while mouse NSph maintain their growth factor dependency for proliferation. For statistical analysis, two-way ANOVA-Bonferroni post hoc test was performed. (**e**) Chromosome preparations for rNSph (*left*) and mNSph (*right*). The karyotype of mNSph seems to be stable and shows only few chromosomal aberrations, such as breaks (*arrow*). In contrast, rNSph low passage cultures are polyploid and show many deletions (*arrowhead*) and breaks (*arrows*). Abbreviations: *GF* Growth Factors

physiological properties using patch clamp techniques. Figure 7a shows typical examples of cells analyzed and confirms the morphological differences of rat and mouse derived NSph: while rNSph had numerous branched processes reminiscent of oligodendroglial progenitors (Fig. 7a, left panel), mNSph were mostly uni- or bipolar (Fig. 7a, right panel). Immediately after attaining a stable whole-cell recording, the resting membrane potentials (Vr) were recorded in current-clamp mode. The resting membrane potential (Vr) of rNSph was less negative than that of mNSph. rNSph had a mean Vr of −58.5±1.2 mV (n=13), whereas the Vr of mNSph was −69.2±1.4 mV (n=9), which is closer to the equilibrium potential for K^+ ($p<$ 0.000006, Fig. 7b).

Electrical stimulation led to activation of different types of voltage-dependent currents. A representative voltage-clamp recording from rNSph is shown in Fig. 7c. In order to analyze the electrophysiological properties of rNSph, membrane potentials were clamped at a holding potential of −40 mV and the cells were depolarized to 50 mV in 10 mV

Table 1 Chromosome numbers of rNSph and mNSph in low/high passage cultures. The karyotype of mNSph shows median chromosome numbers of 40 and 37.2 in low and high passage cultures, respectively, and seems to be more stable compared to rNSph. rNSph low passage cultures are polyploid with a median chromosome number of 67.1, while rNSph high passage cultures are diploid or pseudodiploid with a median chromosome number of 39.5.

	mNSph low passage	mNSph high passage	rNSph low passage	rNSph high passage
median chromosome number ± SD	40.0±10.1	37.2±5.3	67.1±15.4	39.5±7.1

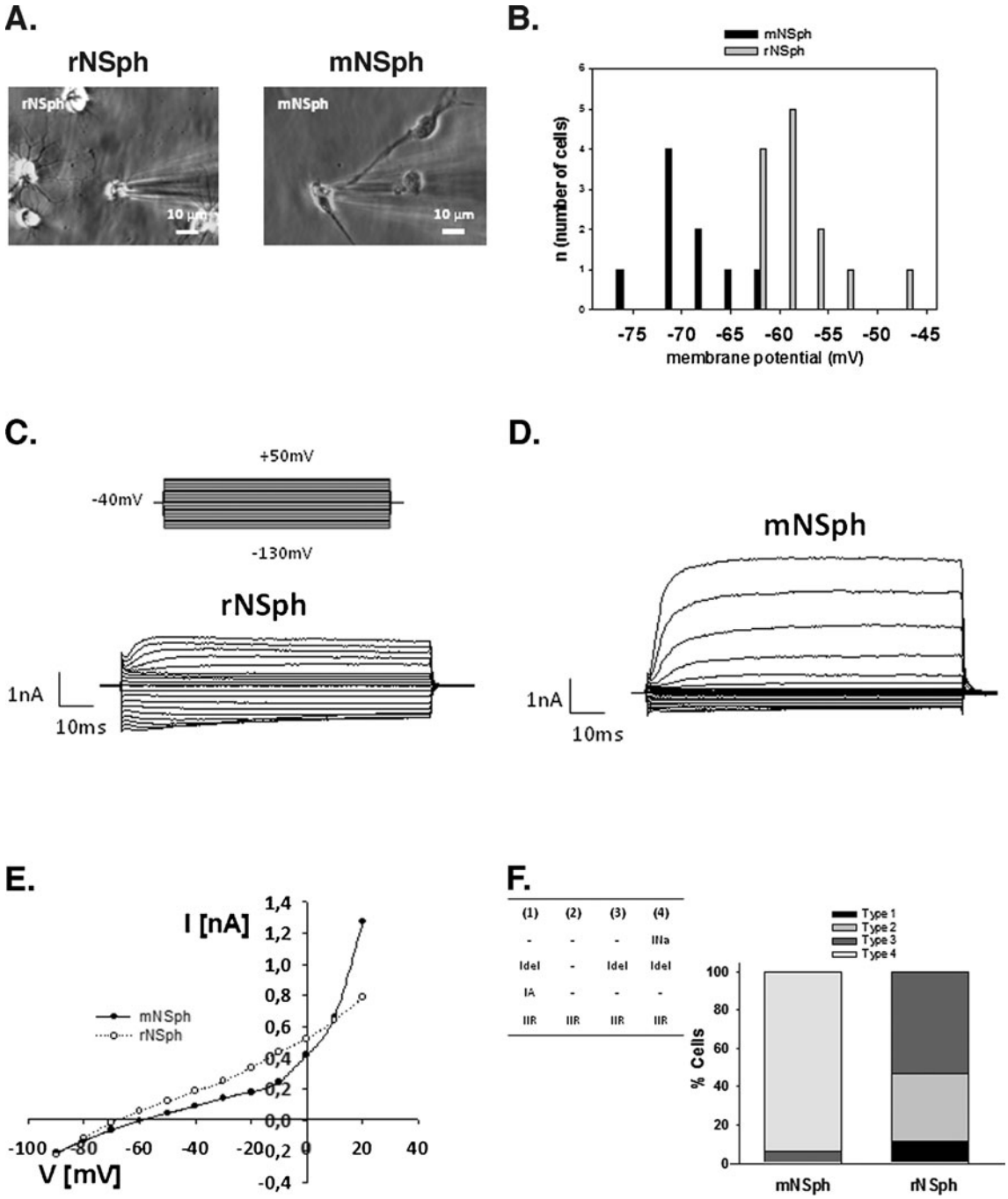

Fig. 7 Comparison of passive and active membrane properties of rNSph and mNSph. (**a**) Morphological characteristics of rNSph as well as mNSph. (**b**) Comparison of the resting potential (V_r) of rNSph and mNSph. mNSph demonstrated resting membrane potentials (RMP) that were significantly more negative (P=0.000006). (**c**) Whole-cell patch clamp analysis of rNSph and mNSph: protocol of electrical stimulation. Membrane potentials were clamped at a holding potential of −40 mV and the cells were depolarized to 90 mV in 10 mV steps in 50 ms followed by −10 mV steps to −90 mV in 50 ms. (**c**, **d**) Representative voltage-clamp recordings from rNSph (**c**) and mNSph (**d**) stimulated with the protocol shown in (**c**). (**e**) Analysis of voltage-dependent activation: steady-state current amplitudes from experiments shown in (**c**) and (**d**) were plotted against the membrane potentials of the electrical stimulation. rNSph showed an almost linear current–voltage relationship. (**f**) Data illustrate the relative contributions of cells subdivided into four groups on the basis of their expression profile of voltage-dependent currents. Currents in the four cell types are listed in the table. l_{Na}: voltage-activated Na^+ currents; I_{del}: delayed rectifier K^+ currents; I_A: *A*-type K^+ currents; l_{IR}: inwardly rectifying K^+ currents

steps in 50 ms followed by −10 mV steps to −130 mV in 50 ms. Cells from rNSph had the typical electrophysiological characteristics of glial cells. They showed almost symmetrical, inwardly and outwardly directed currents

resulting in a linear I-V-relationship (Fig. 7c, e). The cells had a mean outward current density of 221.6±16.8 $pApF^{-1}$ (n=6). The outward current recorded in rNSph (Fig. 7c) revealed the presence of at least two different outward K^+ current subpopulations with different inactivation properties: a delayed rectifier current (no inactivation) and an A-type current (fast inactivation). Moreover, rNSph displayed an inward rectifier current with inactivation at very negative voltages.

A typical whole-cell current pattern from mNSph is shown in Fig. 7d. In contrast to the rNSph, mNSph did not show an inward rectifier K^+ current but had large delayed rectified K^+ currents and inward currents, which were activated by depolarization and were sensitive to 100nM tetrodotoxin (TTX) identifying them as voltage-dependent Na^+ currents. In order to analyze the voltage-dependent activation steady-state current amplitudes from the recordings shown in Fig. 7c, d were plotted against the membrane potentials of the electrical stimulation (Fig. 7e). The IV curves of the rNSph were nearly linear, underlining the oligodendrocyte-like phenotype of rNSph. The IV curves give a reversal potential of −70 mV showing a major contribution of K^+ channels to these currents (Nernst-equilibrium potential for K^+ equals −96 mV). In contrast, the outward current of mNSph is characterized by a large delayed rectifier K^+ current and absence of A-type current. Four cell types can be distinguished as shown in Fig. 7f. The stacked histogram shows the proportions of the four cell types, which could be grouped by their pattern of ion channel subtypes. The majority of the mNSph showed the same physiological properties namely the presence of voltage-gated Na^+ and K^+ channels. mNSph expressed a rapidly activating and inactivating inward current elicited by depolarization to −35 mV and above. These transient inward currents were followed by outwardly rectifying currents with an activation threshold of about −40 mV. In contrast, 1/3 of the rNSph expressed only inwardly rectifying K^+ currents, but neither Na^+ nor other K^+ channels.

To evaluate the expression of ion channels different from K^+ channels, whole-cell recordings were performed under extra- and intracellular K^+-free conditions, occasionally 100 nM TTX was added to the bath solution. A voltage-clamp protocol consisted of depolarising steps from −170 to +10 mV with a 10 mV increment for 50 ms from −80 mV holding potential was used to test for the presence of voltage-dependent Na^+ channels (Fig. 8a). In mNSph depolarizing voltage stimuli elicited a rapidly activating inward current that peaked in 1–2 ms and inactivated within 5 ms (Fig. 8a). This inward current was completely blocked by 100 nM TTX confirming them as voltage-dependent Na^+ currents. All the recorded cells failed to elicit the action potential. The currents activated at potentials more positive than −35 mV (Fig. 8b).

Moreover, rNSph and mNSph displayed a different inward/outward current ratio. The sodium current (I_{Na}) density was remarkably different between mNSph and rNSph. The sodium current density in mNSph was 83.5±9.5 $pApF^{-1}$ (n=7), whereas in rNSph the sodium current density was only 5.6±4.1 $pApF^{-1}$ (n=6) (Fig. 8c). A separate analysis of the inward and outward currents showed that both inward and outward current density were significantly different between mNSph and rNSph (Fig. 8d). mNSph cells had an outward current density of 209.1±21.2 $pApF^{-1}$ (n=8) whereas in rNSph the outward current density was 133.8±29.0 $pApF^{-1}$ (n=12; p<0.03). The inward current density was significant smaller in mNSph (p<0.009).

The Different rNSph and mNSph Cell Identities are Most Likely Not Due to Autocrine Mechanisms

All the experiments described so far used NSph grown in proliferation media containing the human recombinant growth factors EGF and FGF-2. Therefore, we hypothesized that the human growth factors might have different affinities for the mouse and rat EGF- and FGF-2-receptors and in consequence, different cell types or cell lineages might be selected during the culture procedure. Thus, rNSph/mNSph were originated and grown in the presence of human growth factors as control and in the presence of rat/mouse growth factors to analyze whether species specific growth factors change the cell identities of NSph (Fig. 9a, d). After NSph had formed, cell identity, fate and also the response to GFW were determined. We focused on the expression of oligodendrocyte and astrocyte markers, because the neuronal potential of both rat and mouse NSph was relatively low. There was no significant difference in the percentages of O4- or GFAP-positive cells in rat or mouse derived cells depending on the growth factor species (Fig. 9b, e). Moreover, the rat and mouse species differences regarding the percentages of MBP- and GFAP-expressing cells after GFW were retained independently of the species of the growth factors used (Fig. 9c, f). In summary, the differences in identity and fate of cells derived from rNSph versus mNSph are not generated by a different response or selection caused by growth factor species differences.

Next, we analyzed whether the differences in the cell identity of rNSph and mNSph can be explained by an autocrine or paracrine regulation. Thus, either rNSph or mNSph may secret a factor(s) that act in an autocrine or paracrine way to select or induce a specific cell type. Therefore, rNSph and mNSph were incubated with conditioned media derived from NSph from the other species (Fig. 10a, d) to test whether this converts rNSph into mouse-like NSph or mNSph into rat-like NSph.

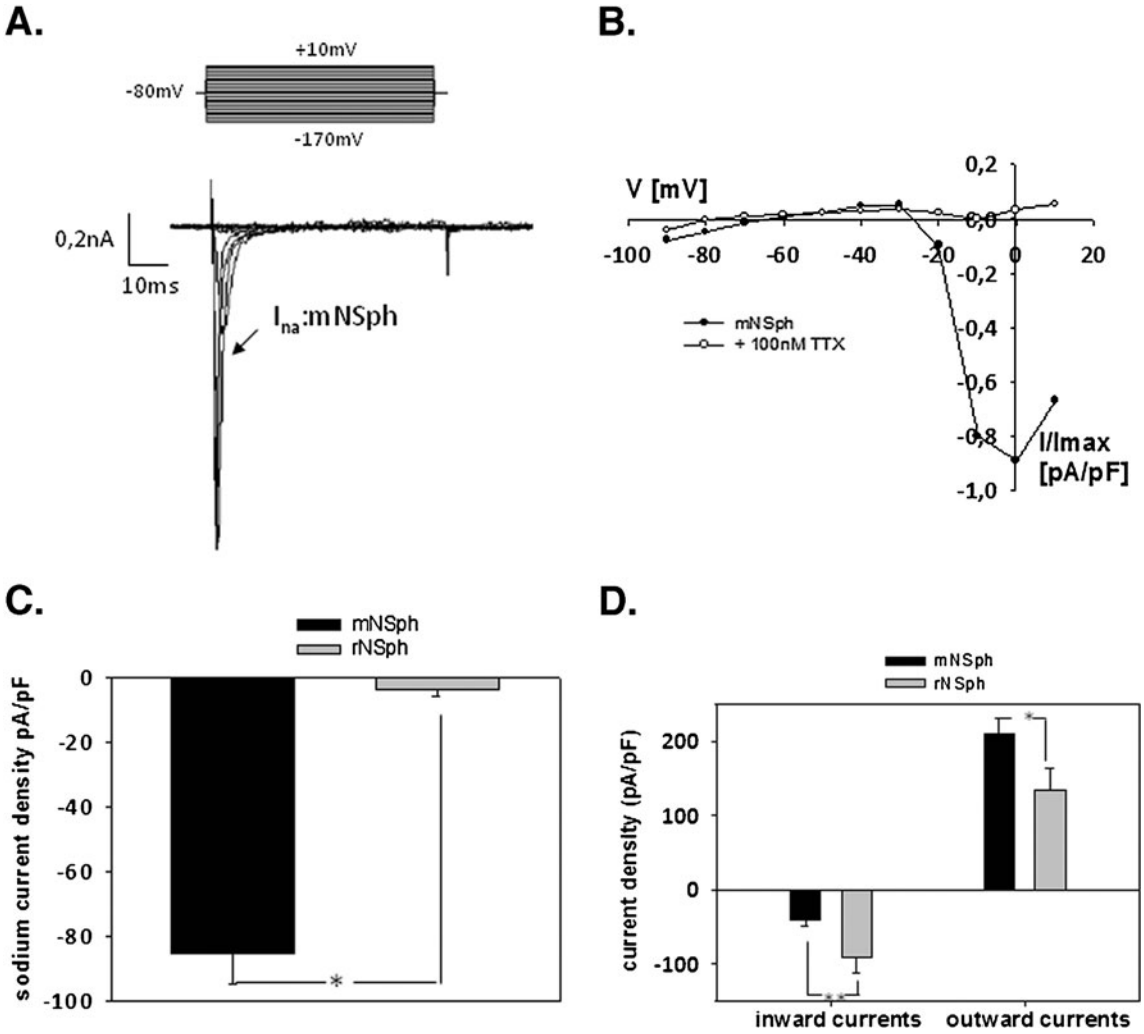

Fig. 8 Voltage-gated sodium currents and comparison of inward and outward current densities. (**a**) To identify voltage-dependent Na^+ channels KCl in the pipette solution was entirely replaced by CsCl and 1 mM Ba^{2+}. Membrane potentials were clamped at a holding potential of −80 mV and the cells were depolarized to 90 mV in 10 mV steps in 50 ms followed by −10 mV steps to −90 mV in 50 ms. (**a**) Representative voltage-clamp recordings of voltage-gated Na^+ channel current (I_{Na}) from mNSph. (**b**) Current–voltage relationship of the peak I_{Na} shown in (**a**) and after addition of 100nM tetrodotoxin (TTX). Addition of 100nM TTX in the bath solution blocked I_{Na} completely. (**c**) Comparison of the current densities of I_{Na} in rNSph and mNSph. Presence of TTX-sensitive voltage-gated Na^+ currents underlying the neuronal-like cell type. (**d**) Comparison of inward and outward current densities in mNSph and rNSph

NSph were incubated for 3 weeks with conditioned media from the other species. Thereafter, cell phenotype and cell fate were analyzed by cell-lineage-specific marker expression and GFW response, respectively. As a result, neither the mNSph-CM nor the rNSph-CM produced a change in the cell identity of the other species. In rNSph, for example, the expression of O4 was not decreased in response to conditioned media from mNSph, and the expression of GFAP was not increased (Fig. 10b). Also, after GFW, rNSph grown in conditioned media from mNSph still gave rise mainly to MBP-expressing mature oligodendrocytes and generated only a minor percentage of GFAP-positive cells (Fig. 10c). Vice versa, the conditioned media from rNSph did neither increase the O4 expression nor decrease the GFAP expression in cells from mNSph (Fig. 10e). Moreover, treated mNSph grown in conditioned media from rNSph mainly gave rise to GFAP-expressing astrocytes, but not to MBP-positive oligodendrocytes after GFW (Fig. 10f). These findings suggest that the species differences in mouse versus rat NSph are probably not caused by auto- or paracrine mechanisms. However, the possibility of species-specific ligand-repector interactions cannot be excluded at this point.

Discussion

Species dependent variations in stem cell populations have recently been described in several studies compar-

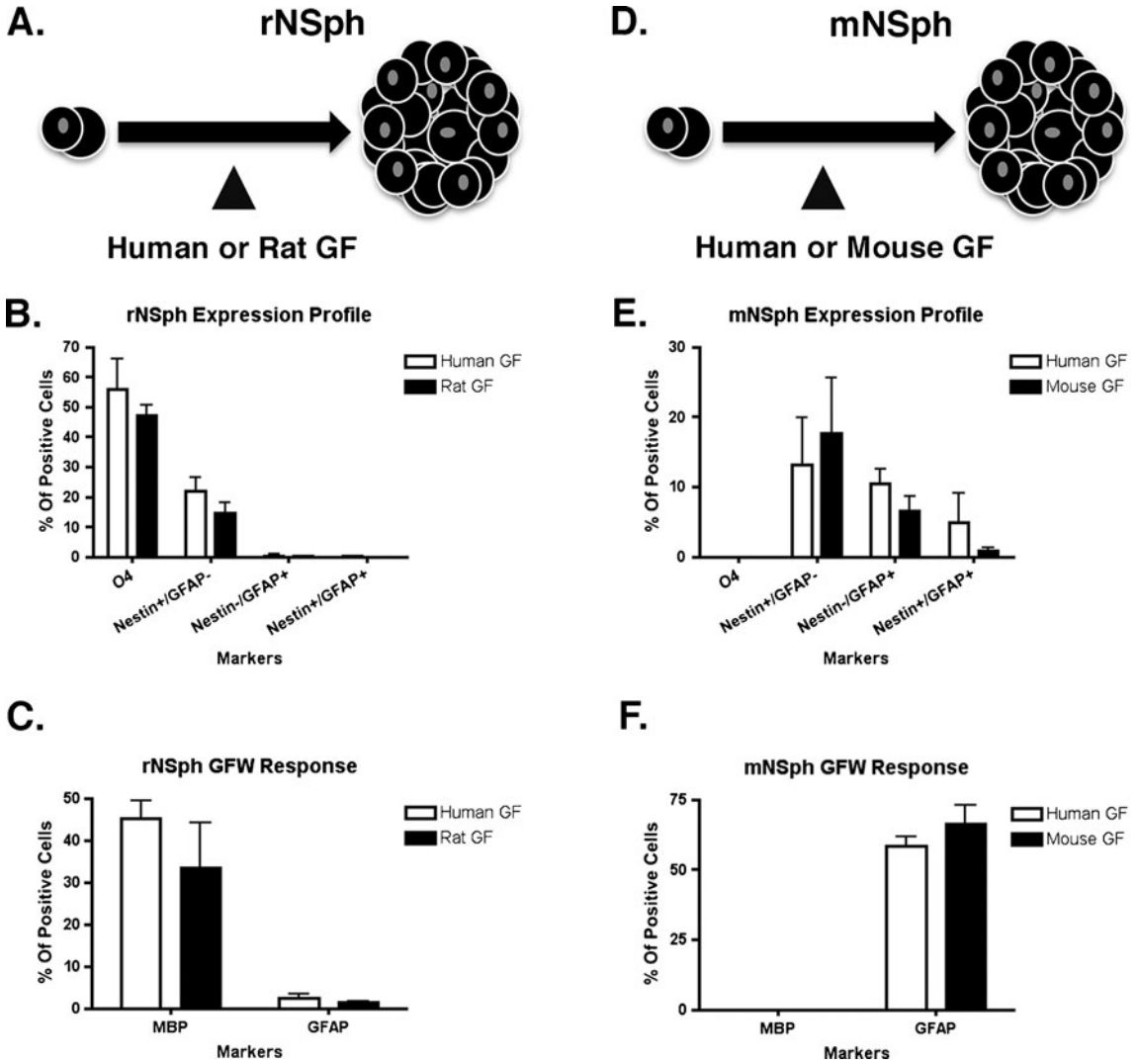

Fig. 9 Cell identity of rNSph and mNSph originated and grown in the presence of growth factors derived from different species. (**a**, **d**) Rat and mouse NSph were generated using growth factors derived from human or, alternatively, from rat and mouse respectively. (**b**, **e**) Quantitative analysis of the cell phenotype analyzed by the expression profile of cell-lineage-specific markers. Note that the percentage of GFAP- and O4-expressing cells is not affected in rNSph (**b**) neither in mNSph (**e**) independently of the growth factors used to generate the different NSph. (**c**, **f**) Quantitative analysis of the cell fate analyzed by the GFW response. The percentage of GFAP- and MBP-expressing cells is not affected in rNSph (**c**) neither in mNSph (**f**) independently of the growth factors used to generate the different NSph. For statistical analysis, two-way ANOVA-Bonferroni post hoc test was performed. Abbreviations: *GFW* growth factor withdrawal

ing mainly human and rodent derived ES cells [24–26]. Here, we demonstrate that there are also considerable differences within the rodent species rat and mouse by characterizing adult NSph cultures from these two species regarding their cell identity, potential and function. Although NSph were prepared and cultured under the exact same conditions mouse and rat derived cells were different i) in their electrophysiological and therefore functional properties, ii) in the expression pattern of cell type specific markers, iii) in their differentiation potential, and iv) in their capability to be protected from transformation after long term passaging.

Identity and Potential of NSph Derived Cells

First of all, the resting potential of rat cells was more positive than the one in mouse cells. Rat cells also showed a significant lower total current density and in contrast to mouse cells an almost linear current/voltage relationship. The fine analysis of the ion channels, which could contribute to such electrophysiological differences, demonstrated the expression of delayed rectifier K^+ channels (slow activation, activation by depolarization to potentials more positive than −30 mV, no inactivation), of inward rectifier channels (fast activation, activation by hyperpolar-

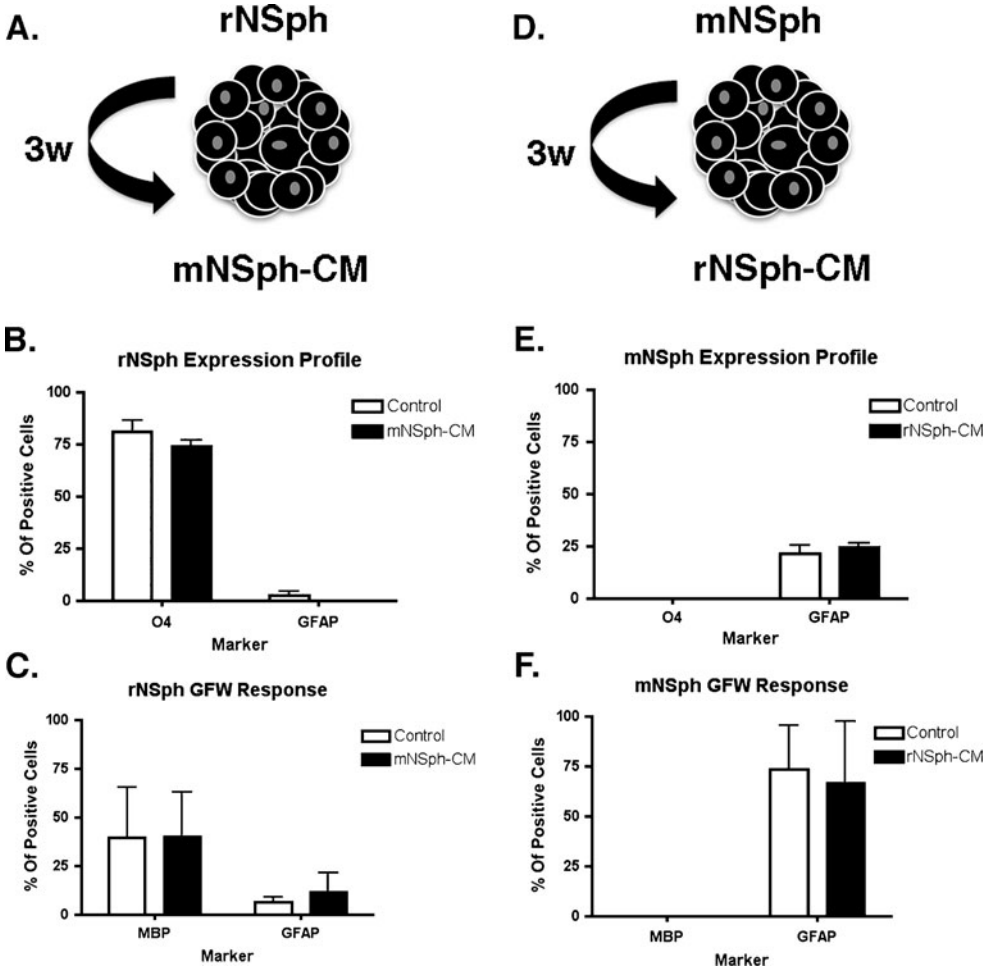

Fig. 10 rNSph and mNSph cell identities can not be changed by NSph conditioned media from the other species. (**a**, **d**) To test whether the observed differences between rNSph and mNSph cell identities are due to an autocrine or paracrine regulation, NSph were incubated for 3 weeks with NSph-CM from the other species. That means rNSph were incubated with mNSph-CM (**a**) and mNSph were incubated with rNSph-CM (**d**). Cell phenotype was analyzed by the expression profile of cell-lineage-specific markers. (**b**, **e**) Quantitative analysis of the cell-lineage-specific marker expression for rNSph (**b**) and mNSph (**e**). The mNSph-CM did neither reduce O4 expression nor increase GFAP expression in rNSph compared to control. Note also that rNSph-CM did not change the expression pattern of mNSph. Cell fate was analyzed by the GFW response. (**c**, **f**) Quantitative analysis of GFW response for rNSph (**c**) and mNSph (**f**). The mNSph-CM did neither reduce MBP expression nor increase GFAP expression in rNSph compared to control. Note also that rNSph-CM did not change the GFW response of mNSph. For statistical analysis, two-way ANOVA-Bonferroni post hoc test was performed. Abbreviations: *GFW* Growth Factor Withdrawal, *NSph-CM* NSph Conditioned Media

ization to potentials more negative that −70 mV, at very negative potentials inactivation), A-type K^+ channels (fast activation, activation by depolarization to potentials more positive than −50 mV, inactivation) and TTX-sensitive Na^+ currents. Thus, we could detect four different types of cells based on the pattern of active ion channels. Type one was found to express delayed rectifier, A-current and inward rectifier; type two expressed inward-rectifier only; type three expressed delayed rectifier and inward rectifier and type four expressed Na^+ channels together with delayed rectifier and inward rectifier channels.

The majority (90%) of cells in mNSph cultures were of type four cells and the remaining 10% of the cells were of type three. Taking their negative resting potentials together with pattern of ion channels into account mNSph derived cells demonstrated a neuronal potential, although the expression of cell type specific markers pointed towards an astroglial/neural stem cell phenotype. Interestingly these cells were not able to generate action potentials in current-clamp experiments. This might be due to the fact that the Na^+ channels in mNSph cells show an unusual activation threshold at very positive membrane voltages (−30 mV). These currents were blocked by TTX, which identifies them as voltage-dependent Na^+ channels. We have no explanation for this phenomenon, but post-translational modifications of Na^+ channels might contribute to that observation. For example, it is known that the activity of Na^+ channels can be modulated by phosphorylation. Especially the

activity of protein kinase C or tyrosine kinase can lead to a strong shift of the activation threshold towards very positive values [43, 44].

In summary, mNSph derived cells are similar to astrocytic stem cells, which express a complex electrophysiological phenotype. Such properties have been described for a subpopulation of Nestin-expressing precursors in the dentate gyrus [45], a subpopulation of CA1 astrocytes [46, 47], but also for oligodendroglial progenitor cells [48]. These "complex astrocytes" are postulated to be an intermediate cell type with glial properties but neuronal potential [47]. Based on our electrophysiological characterization we cannot differentiate whether the neuron-like phenotype of mouse NSph derived cells represents a true neuronal committed pointing towards a restricted precursor cell or whether the cell might still be tripotent and generate all three CNS lineages. The expression pattern of cell type specific markers in mNSph derived cells, at least, indicates an astroglial and a neuronal potential. The majority of the cells expressed Nestin, GFAP and/or A2B5, but almost none of the cells expressed the oligodendroglial precursor O4. They mainly generated GFAP-expressing astrocytes and, upon exposure to neurogenic stimuli, DCX-expressing neurons. In contrast, mNSph derived cells hardly generated oligodendrocytes. Therefore, according to the electrophysiological properties and the expression pattern of cell type specific markers, mNSph derived cells can be considered as astroglial/neuronal stem cells. They are mainly restricted to generate astrocytes and some neurons, but have a very limited capacity to develop oligodendrocytes.

Cells derived form rNSph showed electrophysiologically a more heterogeneous pattern suggesting the presence of different cell types. The cultures consisted of cell type one, two and three, but not of type four, i.e. cells with Na^+ channels, suggesting a glial and not a neuronal cell type. The predominant phenotypes in the culture were cells with either inward rectifier channels only or with inward rectifier and delayed rectifier channels. Thus, most of the rNSph derived cells expressed inward rectifier K^+ channels. This pattern is reminiscent of oligodendroglial lineage cells and corresponds with last stages (stage three and four) of oligodendrocyte development [48]. The expression pattern of cell-type specific markers is consistent with oligodendroglial progenitors in that the majority of rNSph derived cells express A2B5 and O4. Moreover, the cells readily differentiated into oligodendrocytes after GFW or upon stimulation with an oligodendroglial inducing activity. Surprisingly, under proliferation conditions, but not after GFW or upon stimulation with neurogenic stimuli, cells expressed DCX. This is reminiscent of the in vivo situation, where the onset of DCX expression along the ontogeny of a neuron is at the stage of proliferating neuroblasts, while down-regulation of DCX expression correlates with terminal differentiation and integration [49, 50]. Alternatively, the pattern of DCX expression in rNSph derived cells could also suggests that i) the expression of DCX is not as restricted to a neuronal phenotype as previously thought, or ii) the rNSph derived cells might have some neuronal potential, which, under the experimental conditions used, could not be evoked. Apparently, there is a NG2-positive subpopulation of cells in the cortex that co-expresses DCX, actively divides under physiological conditions and generates oligodendrocytes and neurons [51]. Moreover, fate mapping of NG2-positive cells using the proteolipid promoter Cre-strategy demonstrated that NG2-positive cells generate all three CNS lineages, neurons, astrocytes and oligodendrocytes [52]. Here, further experiments are required to delineate the lineage of DCX-expressing cells, but own preliminary data using DCX-CreERT mice indicate a neuronal fate restriction of DCX-positive cells under physiological conditions (Couillard-Despres, unpublished observation).

The Tumor Potential of Different Progenitor Populations

The possibility of neural progenitor cells being at the origin of brain tumor initiating cells triggered an intense search for the identity of the tumor initiating stem cell [53]. This has been evoked by findings that neural stem cell like cells are present in brain tumors, and that these cells can generate new tumors after transplantation [53]. The identity of tumor derived tumor-initiating cells is still under debate, and most likely, it is not one single cell type that can generate brain tumors. Also, along that line, different tumor-initiating cells may produce different types of tumors. For example, medulloblastomas are derived from neural stem cells during brain development [54]. Glioblastomas can be generated from CD133-positive as well as CD133-negative brain tumor stem cells [55]. In addition, the vast majority of brain tumors of the adult brain are generated by progenitors and not by stem cells. For example, the induction of tumors in oligodendroglial progenitors generated gliomas reminiscent of WHO grade II oligodendrogliomas [56]. Moreover, the fact that the majority of brain tumors are found in non-neurogenic regions suggests that progenitors rather than neural stem cells initiate brain tumor formation. The present data demonstrate that rat derived NSph readily transform into growth factor independent tumorigenic cells after extended passaging, while mouse derived NSph retained the growth factor control. This finding is also supported by the observed instability in the karyotype of rNSph, which were polyploid in low passages and (pseudo)diploid in high passages. The same phenomenon has already been found in adult retinal stem cells [57]. High passage cultures from adult retinal stem cells had a tumorigenic potential after subcutaneous transplantation into nude mice. The cells in

the tumor were mainly diploid and pseudodiploid. Thus, cells that were polyploid in low passages seem to undergo a transformation resulting in pseudodiploid cells with tumorigenic potential. This transformation could be due to the loss of cell cycle regulators as a consequence of chromosomal aberrations such as breaks, gaps and deletions in high passage cultures. It should be mentioned that chromosomal abnormalities do not necessarily result in an altered differentiation potential [58, 59], however, the data presented clearly urge for the awareness of the tumor potential of NSPCs. Nevertheless, the fact that rNSph show genetic instabilities and have mainly characteristics of oligodendroglial progenitors in contrast to mNSph, which present mainly astrocytic/neural stem cells, supports the idea that brain tumors unlikely develop from stem cells but from progenitors.

Why are Rat and Mouse Derived NSphs Different?

Although rNSph and mNSph were obtained from the same brain region, i.e. the hippocampus, they displayed different cell identities, potential and function. However, the reason for these differences has yet to be identified. At present, and based on our experiments we can exclude that the observed differences between mouse and rat NSph are due to a specific response to human derived growth factors, since cell phenotypes did not change when cells were stimulated with the species specific derived FGF-2 and EGF. Moreover, most likely we can exclude an autocrine or paracrine mechanism to be responsible for the differences between rNSph and mNSph. However, such hypotheses were only tested for soluble factors that are released by NSph derived cells. Contact-dependant cellular interactions or components from the extracellular matrix might be involved in the species specific phenotypes. Most likely, but still to be proven, hippocampal NSph generating progenitor cells might display differences in their responsiveness to a particular activity present in the culture media. Candidates could be for example the substances present in the B27 supplement. In addition, minor differences in the responsiveness to growth factors such as EGF and/or bFGF could contribute to a selection of specific subpopulations in the NSph cultures [60].

Conclusion

This study is the first attempt to comprehensively compare adult stem/progenitor cells from different rodent species showing that rNSph mainly display an OPC-like identity, while mNSph are composed of a major astrocyte progenitor cell-like population. Taken the observations and the conclusion in consideration, this work strongly encourages for special caution when extrapolating findings from one species to another or to the in vivo situation. This is of particular interest when human derived stem/progenitor cells will be prepared for clinical trials.

Acknowledgements The authors would like to thank the following funding agencies for their support: the Bavarian State Ministry of Sciences, Research and the Arts (ForNeuroCell grant to C.S. and A.-M. P.), the Germany Federal Ministry of Education and Research (BMBF grants #01GG0706, #01GN0979; #0312134; #01GN0505; NGFNplus Brain Tumor Network. Subproject 7 #01GS0887), Alexander von Humboldt Foundation (Georg Forster Program to F.J.R.), Deutsche Forschungsgesellschaft (DFG grant #AI31/3-1, #AI31/4-1) and by the state of Salzburg. We disclose any conflict of interest.

Disclosures The authors indicate no potential conflicts of interest.

References

1. Gage, F. H., Ray, J., & Fisher, L. J. (1995). Isolation, characterization, and use of stem cells from the CNS. *Annual Review of Neuroscience, 18*, 159–192.
2. Palmer, T. D., Markakis, E. A., Willhoite, A. R., Safar, F., & Gage, F. H. (1999). Fibroblast Growth Factor-2 Activates a Latent Neurogenic Program in Neural Stem Cells from Diverse Regions of the Adult CNS. *The Journal of Neuroscience, 19*, 8487–8497.
3. Palmer, T. D., Ray, J., & Gage, F. H. (1995). FGF-2-Responsive Neuronal Progenitors Reside in Proliferative and Quiescent Regions of the Adult Rodent Brain. *Molecular and Cellular Neuroscience, 6*, 474–486.
4. Reynolds, B. A., & Weiss, S. (1992). Generation of Neurons and Astrocytes from Isolated Cells of the Adult Mammalian Central-Nervous-System. *Science, 255*, 1707–1710.
5. Wachs, F. P., Couillard-Despres, S., Engelhardt, M., et al. (2003). High efficacy of clonal growth and expansion of adult neural stem cells. *Laboratory Investigation, 83*, 949–962.
6. Reynolds, B. A., & Rietze, R. L. (2005). Neural stem cells and neurospheres–re-evaluating the relationship. *Natural Methods, 2*, 333–336.
7. Gritti, A., Parati, E. A., Cova, L., et al. (1996). Multipotential stem cells from the adult mouse brain proliferate and self-renew in response to basic fibroblast growth factor. *The Journal of Neuroscience, 16*, 1091–1100.
8. Johe, K. K., Hazel, T. G., Muller, T., Dugich-Djordjevic, M. M., & McKay, R. D. (1996). Single factors direct the differentiation of stem cells from the fetal and adult central nervous system. *Genes & Development, 10*, 3129–3140.
9. Takahashi, J., Palmer, T. D., & Gage, F. H. (1999). Retinoic acid and neurotrophins collaborate to regulate neurogenesis in adult-derived neural stem cell cultures. *Journal of Neurobiology, 38*, 65–81.
10. Gross, R. E., Mehler, M. F., Mabie, P. C., Zang, Z., Santschi, L., & Kessler, J. A. (1996). Bone Morphogenetic Proteins Promote Astroglial Lineage Commitment by Mammalian Subventricular Zone Progenitor Cells. *Neuron, 17*, 595–606.
11. Nakashima, K., Yanagisawa, M., Arakawa, H., & Taga, T. (1999). Astrocyte differentiation mediated by LIF in cooperation with BMP2. *FEBS Letters, 457*, 43–46.
12. Hsieh, J., Aimone, J. B., Kaspar, B. K., Kuwabara, T., Nakashima, K., & Gage, F. H. (2004). IGF-I instructs multipotent adult neural progenitor cells to become oligodendrocytes. *The Journal of Cell Biology, 164*, 111–122.

13. Rivera, F. J., Couillard-Despres, S., Pedre, X., et al. (2006). Mesenchymal Stem Cells Instruct Oligodendrogenic Fate Decision on Adult Neural Stem Cells. *Stem Cells, 24*, 2209–2219.
14. Gage, F. H. (2000). Mammalian Neural Stem Cells. *Science, 287*, 1433–1438.
15. Eriksson, P. S., Perfilieva, E., Bjork-Eriksson, T., et al. (1998). Neurogenesis in the adult human hippocampus. *Natural Medicines, 4*, 1313–1317.
16. Snyder, J. S., Choe, J. S., Clifford, M. A., et al. (2009). Adult-born hippocampal neurons are more numerous, faster maturing, and more involved in behavior in rats than in mice. *The Journal of Neuroscience, 29*, 14484–14495.
17. Gil-Mohapel, J., Simpson, J. M., Titterness, A. K., & Christie, B. R. (2010). Characterization of the neurogenesis quiescent zone in the rodent brain: Effects of age and exercise. *The European Journal of Neuroscience, 31*, 797–807.
18. Melvin, N. R., Spanswick, S. C., Lehmann, H., & Sutherland, R. J. (2007). Differential neurogenesis in the adult rat dentate gyrus: An identifiable zone that consistently lacks neurogenesis. *The European Journal of Neuroscience, 25*, 1023–1029.
19. Dziembowska, M., Tham, T. N., Lau, P., Vitry, S., Lazarini, F., & Dubois-Dalcq, M. (2005). A role for CXCR4 signaling in survival and migration of neural and oligodendrocyte precursors. *Glia, 50*, 258–269.
20. Gong, X., He, X., Qi, L., Zuo, H., & Xie, Z. (2006). Stromal cell derived factor-1 acutely promotes neural progenitor cell proliferation in vitro by a mechanism involving the ERK1/2 and PI-3 K signal pathways. *Cell Biology International, 30*, 466–471.
21. Bauer, S., & Patterson, P. H. (2006). Leukemia inhibitory factor promotes neural stem cell self-renewal in the adult brain. *The Journal of Neuroscience, 26*, 12089–12099.
22. Dictus, C., Tronnier, V., Unterberg, A., & Herold-Mende, C. (2007). Comparative analysis of in vitro conditions for rat adult neural progenitor cells. *Journal of Neuroscience Methods, 161*, 250–258.
23. Ray, J., & Gage, F. H. (2006). Differential properties of adult rat and mouse brain-derived neural stem/progenitor cells. *Molecular and Cellular Neurosciences, 31*, 560–573.
24. Ginis, I., & Rao, M. S. (2003). Toward cell replacement therapy: Promises and caveats. *Experimental Neurology, 184*, 61–77.
25. Ginis, I., Luo, Y., Miura, T., et al. (2004). Differences between human and mouse embryonic stem cells. *Developmental Biology, 269*, 360–380.
26. Rao, M. (2004). Conserved and divergent paths that regulate self-renewal in mouse and human embryonic stem cells. *Developmental Biology, 275*, 269–286.
27. Theise, N. D. (2005). On experimental design and discourse in plasticity research. *Stem Cell Reviews, 1*, 9–13.
28. Glover, J. C., Boulland, J. L., Halasi, G., & Kasumacic, N. (2009). Chimeric animal models in human stem cell biology. *ILAR Journal, 51*, 62–73.
29. Endl, E., Steinbach, P., Knuchel, R., & Hofstadter, F. (1997). Analysis of cell cycle-related Ki-67 and p120 expression by flow cytometric BrdUrd-Hoechst/7AAD and immunolabeling technique. *Cytometry, 29*, 233–241.
30. Amit, M., Carpenter, M. K., Inokuma, M. S., et al. (2000). Clonally derived human embryonic stem cell lines maintain pluripotency and proliferative potential for prolonged periods of culture. *Developmental Biology, 227*, 271–278.
31. Cheng, J., Dutra, A., Takesono, A., Garrett-Beal, L., & Schwartzberg, P. L. (2004). Improved generation of C57BL/6 J mouse embryonic stem cells in a defined serum-free media. *Genesis, 39*, 100–104.
32. Smith, A. G., Heath, J. K., Donaldson, D. D., et al. (1988). Inhibition of pluripotential embryonic stem cell differentiation by purified polypeptides. *Nature, 336*, 688–690.
33. Livak, K. J., & Schmittgen, T. D. (2001). Analysis of relative gene expression data using real-time quantitative PCR and the 2(−Delta Delta C(T)) Method. *Methods, 25*, 402–408.
34. Raff, M. C. (1984). Williams BPa, Miller RH. The in vitro differentiation of a bipotential glial progenitor cell. *The EMBO Journal, 3*, 1857–1864.
35. Ahlgren, S. C., Wallace, H., Bishop, J., Neophytou, C., & Raff, M. C. (1997). Effects of Thyroid Hormone on Embryonic Oligodendrocyte Precursor Cell Developmentin Vivoandin Vitro. *Molecular and Cellular Neuroscience, 9*, 420–432.
36. Calver, A. R., Hall, A. C., Yu, W.-P., et al. (1998). Oligodendrocyte Population Dynamics and the Role of PDGF In Vivo. *Neuron, 20*, 869–882.
37. Davies, J. E., & Miller, R. H. (2001). Local Sonic Hedgehog Signaling Regulates Oligodendrocyte Precursor Appearance in Multiple Ventricular Zone Domains in the Chick Metencephalon. *Developmental Biology, 233*, 513–525.
38. Fruttiger, M., Karlsson, L., Hall, A. C., et al. (1999). Defective oligodendrocyte development and severe hypomyelination in PDGF-A knockout mice. *Development, 126*, 457–467.
39. Koper, J., Hoeben, R., Hochstenbach, F., van Golde, L., & Lopes-Cardozo, M. (1986). Effects of triiodothyronine on the synthesis of sulfolipids by oligodendrocyte-enriched glial cultures. *Biochimica et Biophysica Acta, 887*, 327–334.
40. Samanta, J., & Kessler, J. A. (2004). Interactions between ID and OLIG proteins mediate the inhibitory effects of BMP4 on oligodendroglial differentiation. *Development, 131*, 4131–4142.
41. Zhu, G., Mehler, M. F., & Zhao, J. (1999). Yu Yung S, Kessler JA. Sonic Hedgehog and BMP2 Exert Opposing Actions on Proliferation and Differentiation of Embryonic Neural Progenitor Cells. *Developmental Biology, 215*, 118–129.
42. Siebzehnrubl, F. A., Jeske, I., Muller, D., et al. (2009). Spontaneous in vitro transformation of adult neural precursors into stem-like cancer cells. *Brain Pathology, 19*, 399–408.
43. Dascal, N., & Lotan, I. (1991). Activation of protein kinase C alters voltage dependence of a Na + channel. *Neuron, 6*, 165–175.
44. Jia, Z., Jia, Y., Liu, B., et al. (2008). Genistein inhibits voltage-gated sodium currents in SCG neurons through protein tyrosine kinase-dependent and kinase-independent mechanisms. *Pflugers Arch European Journal of Physiology, 456*, 857–866.
45. Filippov, V., Kronenberg, G., Pivneva, T., et al. (2003). Subpopulation of nestin-expressing progenitor cells in the adult murine hippocampus shows electrophysiological and morphological characteristics of astrocytes. *Molecular and Cellular Neurosciences, 23*, 373–382.
46. Kronenberg, G., Wang, L. P., Geraerts, M., et al. (2007). Local origin and activity-dependent generation of nestin-expressing protoplasmic astrocytes in CA1. *Brain Structure & Function, 212*, 19–35.
47. Matthias, K., Kirchhoff, F., Seifert, G., et al. (2003). Segregated expression of AMPA-type glutamate receptors and glutamate transporters defines distinct astrocyte populations in the mouse hippocampus. *The Journal of Neuroscience, 23*, 1750–1758.
48. Sontheimer, H., Perouansky, M., Hoppe, D., Lux, H. D., Grantyn, R., & Kettenmann, H. (1989). Glial cells of the oligodendrocyte lineage express proton-activated Na + channels. *Journal of Neuroscience Research, 24*, 496–500.
49. Brown, J. P., Couillard-Despres, S., Cooper-Kuhn, C. M., Winkler, J., Aigner, L., & Kuhn, H. G. (2003). Transient expression of doublecortin during adult neurogenesis. *The Journal of Comparative Neurology, 467*, 1–10.
50. Couillard-Despres, S., Winner, B., Schaubeck, S., et al. (2005). Doublecortin expression levels in adult brain reflect neurogenesis. *The European Journal of Neuroscience, 21*, 1–14.
51. Tamura, Y., Kataoka, Y., Cui, Y., Takamori, Y., Watanabe, Y., & Yamada, H. (2007). Multi-directional differentiation of

doublecortin- and NG2-immunopositive progenitor cells in the adult rat neocortex in vivo. *The European Journal of Neuroscience, 25*, 3489–3498.
52. Guo, F., Ma, J., McCauley, E., Bannerman, P., & Pleasure, D. (2009). Early postnatal proteolipid promoter-expressing progenitors produce multilineage cells in vivo. *The Journal of Neuroscience, 29*, 7256–7270.
53. Singh, S. K., Hawkins, C., Clarke, I. D., et al. (2004). Identification of human brain tumour initiating cells. *Nature, 432*, 396–401.
54. Sutter, R., Shakhova, O., Bhagat, H., et al. (2010). Cerebellar stem cells act as medulloblastoma-initiating cells in a mouse model and a neural stem cell signature characterizes a subset of human medulloblastomas. *Oncogene, 29*, 1845–1856.
55. Beier, D., Hau, P., Proescholdt, M., et al. (2007). CD133(+) and CD133(−) glioblastoma-derived cancer stem cells show differential growth characteristics and molecular profiles. *Cancer Research, 67*, 4010–4015.
56. Lindberg, N., Kastemar, M., Olofsson, T., Smits, A., & Uhrbom, L. (2009). Oligodendrocyte progenitor cells can act as cell of origin for experimental glioma. *Oncogene, 28*, 2266–2275.
57. Djojosubroto, M., Bollotte, F., Wirapati, P., Radtke, F., Stamenkovic, I., & Arsenijevic, Y. (2009). Chromosomal number aberrations and transformation in adult mouse retinal stem cells in vitro. *Investigative Ophthalmology Visual Science, 50*, 5975–5987.
58. McBurney, M. W. (1976). Clonal lines of teratocarcinoma cells in vitro: Differentiation and cytogenetic characteristics. *Journal of Cellular Physiology, 89*, 441–455.
59. Park, J., Yoshida, I., Tada, T., Takagi, N., Takahashi, Y., & Kanagawa, H. (1998). Trisomy 8 does not affect differentiative potential in a murine parthenogenetic embryonic stem cell line. *The Japanese Journal of Veterinary Research, 46*, 29–35.
60. Ray, J., & Gage, F. H. (2006). Differential properties of adult rat and mouse brain-derived neural stem/progenitor cells. *Molecular and Cellular Neuroscience, 31*, 560–573.